© 2014. Published by The Company of Biologists Ltd | Journal of Cell Science (2014) 127, 2723–2735 doi:10.1242/jcs.143644

RESEARCH ARTICLE

Expression of endoglin isoforms in the myeloid lineage and their role during aging and macrophage polarization

Mikel Aristorena[1,2], Francisco J. Blanco[1,2], Mateo de Las Casas-Engel[1], Luisa Ojeda-Fernandez[1,2], Eunate Gallardo-Vara[1,2], Angel Corbi[1], Luisa M. Botella[1,2] and Carmelo Bernabeu[1,2,*]

ABSTRACT

Endoglin plays a crucial role in pathophysiological processes such as hereditary hemorrhagic telangiectasia (HHT), preeclampsia and cancer. Endoglin expression is upregulated during the monocyte-to-macrophage transition, but little is known about its regulation and function in these immune cells. Two different alternatively spliced isoforms of endoglin have been reported, L-endoglin and S-endoglin. Although L-endoglin is the predominant variant, here, we found that there was an increased expression of the S-endoglin isoform during senescence of the myeloid lineage in human and murine models. We performed a stable isotope labelling of amino acids in cell culture (SILAC) analysis of both L-endoglin and S-endoglin transfectants in the human promonocytic cell line U937. Analysis of differentially expressed protein clusters allowed the identification of cellular activities affected during aging. S-endoglin expression led to decreased cellular proliferation and a decreased survival response to granulocyte-macrophage colony-stimulating factor (GM-CSF)-induced apoptosis, as well as increased oxidative stress. Gene expression and functional studies suggested that there was a non-redundant role for each endoglin isoform in monocyte biology. In addition, we found that S-endoglin impairs the monocytic differentiation into the pro-inflammatory M1 phenotype and contributes to the compromised status of macrophage functions during aging.

KEY WORDS: Cellular senescence, Macrophage, Endoglin, Macrophage polarization, Aging, SILAC

INTRODUCTION

Endoglin (also known as CD105) is a type I homodimeric transmembrane glycoprotein that can act as an auxiliary receptor for members of the TGF-β superfamily (Cheifetz et al., 1992; Bellón et al., 1993). Structurally, endoglin belongs to the zona pellucida (ZP) family of proteins that share a ZP domain of ~260 amino acid residues at their juxtamembrane extracellular region (Llorca et al., 2007). Endoglin also contains, at its N-terminal extracellular region, an orphan domain, comprising ~325 amino acids whose sequence is not homologous to any other protein; however, this domain has recently been identified as the minimal active endoglin domain needed for partner recognition (Llorca et al., 2007; Castonguay et al., 2011; Alt et al., 2012).

[1]Centro de Investigaciones Biológicas, Consejo Superior de Investigaciones Científicas (CSIC), 28040 Madrid, Spain. [2]Centro de Investigación Biomédica en Red de Enfermedades Raras (CIBERER), 28040 Madrid, Spain.

*Author for correspondence (bernabeu.c@cib.csic.es)

Received 29 September 2013; Accepted 17 March 2014

Endoglin expression and function has been widely described in the context of endothelial cells and vascular physiology (Bernabeu et al., 2007; López-Novoa and Bernabeu, 2010), playing a key role in many pathological processes, including hereditary hemorrhagic telangiectasia (HHT), cancer angiogenesis, preeclampsia or hypertension (Bernabeu et al., 2009; Shovlin, 2010; Kapur et al., 2012; Rana et al., 2012; Valbuena-Diez et al., 2012). In addition, increased levels of the membrane and soluble forms of endoglin have been linked to inflammatory processes, such as wound healing, atherosclerosis, psoriasis and rheumatoid arthritis (Rulo et al., 1995; Conley et al., 2000; Torsney et al., 2002; López-Novoa and Bernabeu, 2010).

There are two different isoforms of endoglin that share an identical extracellular domain but differ from each other in the length and composition of their cytoplasmic tail (Cheifetz et al., 1992; Bellón et al., 1993). The endoglin gene (*ENG*) is predominantly expressed as a long isoform (L-endoglin), but its pre-mRNA can be alternatively spliced by a mechanism of intron retention, yielding a less abundant form, known as short endoglin (S-endoglin). This intron retention is driven by the SRSF1 splicing factor, which physically competes with the minor spliceosome for the elimination of the last intron between exons 13 and 14 (Blanco and Bernabeu, 2011; Blanco and Bernabeu, 2012). When transcribed, the last intron of *ENG* bears an early stop codon that affects the open reading frame and truncates the mature protein at the cytoplasmic region (Blanco et al., 2008). So far, most studies published about endoglin have focused on L-endoglin. The expression of the short variant (S-endoglin) was first described in humans (Bellón et al., 1993) and later in mice (Pérez-Gómez et al., 2005). Specific transcripts for L-endoglin and S-endoglin have been detected in placenta, lung, heart, epidermis and liver, as well as in epithelial, endothelial and monocytic cells (Bellón et al., 1993; Pérez-Gómez et al., 2005). The cytoplasmic region of human L-endoglin is composed of 47 amino acids with a high content of serine and threonine residues that are susceptible to phosphorylation (Lastres et al., 1994). In addition, the sequence Ser-Met-Ala (SMA) in the C-terminal end of L-endoglin is a docking site for proteins with a PDZ domain and is involved in cytoskeleton organization (Koleva et al., 2006). By contrast, the sequence of the S-endoglin cytoplasmic tail is only 14 amino acids long, the last seven residues being specific for this isoform. These structural differences might account for the distinct functional effects of L-endoglin and S-endoglin (Blanco et al., 2008; Velasco et al., 2008).

Interestingly, a role for S-endoglin during endothelial senescence has been described (Blanco et al., 2008). Thus, the S-endoglin:L-endoglin ratio is increased during senescence of human endothelial cells *in vitro*, as well as during aging of mice in vascularized tissues. The switch between L-endoglin and S-endoglin affects the TGF-β-mediated cell signalling, promoting

Journal of Cell Science (2014) 127, 2723–2735 doi:10.1242/jcs.143644

the ALK5 (TGFBR1)–Smad3 pathway instead of the ALK1 (ACVRL1)–Smad1 route. This is due to the preferential affinity of the short cytoplasmic domain for ALK5, which promotes the expression of target genes such as *SERPINE1* (PAI-1) and *PTGS2* (cyclooxygenase-2, COX-2) and inhibits *NOS3* (nitric oxide synthase 3, eNOS). Furthermore, transgenic mice overexpressing S-endoglin show hypertension, a decreased hypertensive response to NO inhibition, a decreased vasodilatory response to TGF-β1 administration and decreased eNOS expression in lungs and kidneys, supporting the involvement of S-endoglin in the NO-dependent vascular homeostasis (Blanco et al., 2008). Taken together, these results suggest that S-endoglin is induced during endothelial senescence and that it might contribute to age-dependent vascular pathology.

During aging, immune and inflammatory responses are impaired in a general immunosenescence process where macrophage functions are compromised (Cassado Ados et al., 2011; Mahbub et al., 2012). Aged macrophages show reduced functional activity, leading to accumulation of unphagocytosed cellular debris, chronic inflammation and exacerbation of tissue damage and aging (Shaw et al., 2010; Li, 2013). Two physically and functionally distinct macrophage subsets have been described in the mouse peritoneal cavity (Ghosn et al., 2010), which represent different senescence stages. Thus, the long-term resident large peritoneal macrophages (LPMs) exhibit morphological and functional characteristics described in senescent cells, including large size, prominent vacuolization, reduced phagocytic capacity and low expression of MHC class II molecules. In steady-state conditions, >90% of peritoneal macrophages are LPMs and the remaining ones are small peritoneal macrophages (SPMs, young macrophages derived from newly recruited blood monocytes). Upon inflammatory stimuli, the loss of LPMs correlates with the cell renewal of the peritoneal cavity, which is characterized by the enrichment of SPMs. All these data suggest that the peritoneal cavity is a useful tool to analyse macrophage immunosenescence in these two cell subsets (Cassado Ados et al., 2011). Macrophages participate in the immune response according to a preferential M1 or M2 polarization, which is involved not only in the response to pathogens, tumour progression and angiogenesis, but also in tissue homeostasis, autoimmunity and fibrosis (Sunderkötter et al., 1994; Werner and Alzheimer, 2006; Benoit et al., 2008). Although many studies on endoglin have focused on endothelial cells, endoglin expression has also been detected in some myeloid precursors and macrophages. Thus, endoglin acts as a crucial regulator of hematopoietic development, in part by modulating the signalling involving members of the TGF-β superfamily (Borges et al., 2012). Later in development, endoglin is present at low levels on monocytes, but it is markedly upregulated during the monocyte–macrophage transition (Lastres et al., 1992; O'Connell et al., 1992). Moreover, in the human monocytic line U937, ectopic expression of endoglin counteracts TGF-β1-dependent cellular responses (Lastres et al., 1996). Overall, the role of endoglin in the myeloid lineage is poorly understood, especially regarding the individual function of each isoform. Although endoglin expression in human macrophages has been detected in several tissues (Lastres et al., 1992; O'Connell et al., 1992), nothing is known about the regulation and function of the individual endoglin isoforms in macrophages or their contribution to disease. Here, we show that S-endoglin is a marker of macrophage senescence, and both endoglin isoforms contribute to the monocyte-to-macrophage transition and polarization during immunosenescence, thus modulating the system responses due to aging.

RESULTS

Transcript expression of endoglin isoforms in monocytes and macrophages

Endoglin is expressed at low levels on monocytes, but it is markedly upregulated during the monocyte–macrophage transition (Lastres et al., 1992; O'Connell et al., 1992). Both L-endoglin and S-endoglin isoforms have been detected in monocytic cell lines treated with phorbol esters (Bellon et al., 1993), but the regulation of these isoforms in primary cultures of macrophages has not been studied. Because S-endoglin is a marker of cellular senescence (Blanco et al., 2008), we assessed the mRNA expression of both endoglin isoforms in monocytes and macrophages with a senescence-like stage that were subjected to oxidative stress. First, macrophages were obtained from the peritoneal cavity of 2-month-old mice. Most of these cells correspond to the myeloid lineage, mainly to tissue-resident LPMs (Cassado Ados et al., 2011). As a biomarker of macrophage senescence, we used β-galactosidase activity (Cassado Ados et al., 2011). A large proportion of the LPMs were positive for the senescence-associated β-galactosidase staining (Fig. 1A) and there was a marked increase in the percentage of senescent macrophages after hydrogen peroxide (H_2O_2) treatment (Fig. 1B). In addition, increased levels of S-endoglin were observed upon oxidative stress, as shown by semi-quantitative RT-PCR analysis of endoglin transcripts (Fig. 1C). In addition, oxidative-stress-induced senescence in activated monocytes from four human different donors demonstrated a clear increase in the transcript levels of the senescence markers S-endoglin and PAI-1, whereas L-endoglin levels underwent a much lower increase (Fig. 1D). Zymosan particles prepared from yeast cell walls (*Saccharomyces cerevisiae*) and their intraperitoneal injection in mice is commonly used to enrich the peritoneal cavity in macrophages. To assess the effect of *in vivo* aging, LPMs and recruited SPMs were analysed upon zymosan treatment (Fig. 1E,F). S-endoglin levels were clearly increased in both LPMs and SPMs in mice that were 6 and 12 months old (up to 16-fold), relative to 2-month-old animals. Moreover, the senescence marker PAI-1 showed a statistically significant increase in LPMs (at 12 months), whereas L-endoglin transcript levels were augmented in LPMs (at 6 and 12 months) and SPMs (at 12 months), although at lower levels than S-endoglin. Of note, the upregulation of S-endoglin preceded that of PAI-1 in LPMs (Fig. 1E), and no significant changes of PAI-1 levels in infiltrating SPMs during aging were observed (Fig. 1F). Unfortunately, there are no appropriate antibodies able to distinguish between L-endoglin and S-endoglin proteins for these studies. Human S-endoglin and L-endoglin proteins vary from each other in their cytoplasmic tails that contain 14 and 47 amino acids, respectively, with only a sequence of seven residues being specific for S-endoglin (López-Novoa and Bernabeu, 2010). Similar differences are also present in murine endoglin isoforms. These small structural differences explain the lack of appropriate tools to clearly distinguish between L-endoglin and S-endoglin proteins. Taken together, these results suggest that S-endoglin is a marker of macrophage senescence that is upregulated during *in vitro* oxidative-stress-induced senescence and *in vivo* aging.

Identification of differentially expressed proteins in monocytic endoglin transfectants

To assess the impact of the two endoglin isoforms in the monocytic proteome, stable transfectants of U937 cells overexpressing human

Journal of Cell Science (2014) 127, 2723–2735 doi:10.1242/jcs.143644

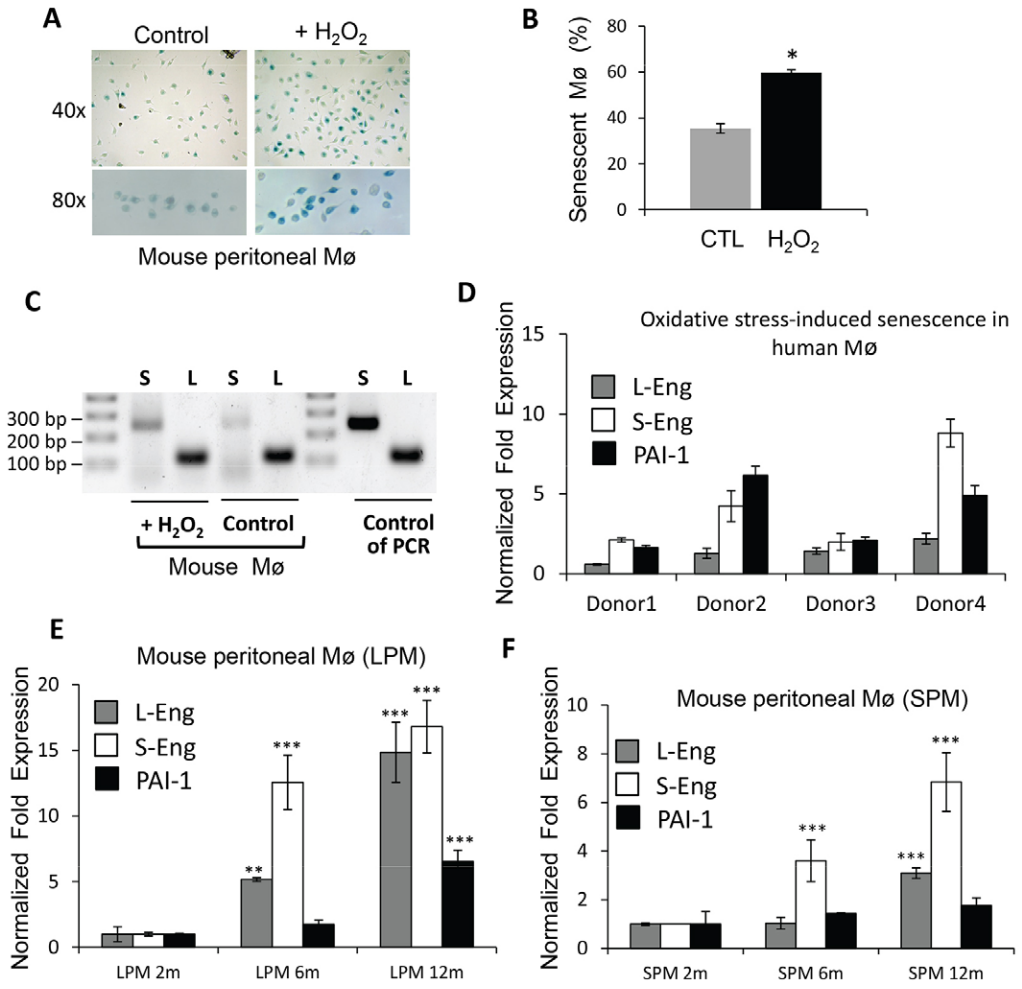

Fig. 1. Expression of endoglin isoforms in monocytes and macrophages upon oxidative-stress-induced senescence and during aging. (A–C) Oxidative-stress-induced senescence in mouse peritoneal macrophages (Mø). Resident LPMs obtained from the peritoneal cavity of 2-month-old mice were incubated in the absence or the presence of hydrogen peroxide (150 μM H_2O_2) for 1 h and stained for the senescence-associated β-galactosidase activity (A). The positivity for this marker is significantly higher in H_2O_2-treated cells compared to controls (B). Cells cultured under oxidative stress conditions present higher levels of S-endoglin than untreated cells, as shown by semi-quantitative RT-PCR; S, S-endoglin; L, L-endoglin (C). (D) Quantitative PCR of oxidative stress-induced senescent human macrophages. Human monocytes were purified from PBMCs by magnetic cell sorting using anti-CD14 and were cultured for 3 days. Adherent cells were incubated in the absence or the presence of 150 μM H_2O_2 and transcript levels were measured. Results are expressed as fold-induction values with respect to untreated cells. Upon oxidative stress, activated monocytes show an increase in both S-endoglin and PAI-1 senescence markers. (E,F) Effect of aging on large and small mouse peritoneal macrophages. Mouse LPMs and SPMs were isolated from untreated (E) and zymosan-treated (F) animals, respectively. Cells were collected from 2-month-old (2m), 6-month-old (6m) and 12-month-old (12m) old mice. Total RNA was extracted and subjected to quantitative RT-PCR to measure S-endoglin (S-Eng), L-endoglin (L-Eng) or PAI-1 transcript levels. Results were normalized to those in 2-month-old animals. Increased levels of S-endoglin in both LPM and newly recruited SPM (due to zymosan) were observed. The statistical significance of 6-month and 12-month samples with respect to 2-month-old mice are indicated. *$P<0.05$; **$P<0.01$; ***$P<0.001$.

L-endoglin or S-endoglin, as well as mock transfectants, were used (Lastres et al., 1996). Although this experimental approach does not necessarily reflect the *in vivo* situation, it represents a useful tool to specifically dissect the individual contribution of endoglin. Protein expression of both endoglin isoforms is markedly enhanced in respect to the basal levels of mock transfectants, as shown by immunofluorescence flow cytometry (Fig. 2A). The presence of L-endoglin and S-endoglin transcripts could be detected by qualitative RT-PCR analysis in all transfectants (Fig. 2B). Proteomics analysis using stable isotope labelling of amino acids in cell culture (SILAC) technology was applied to quantify differences in protein expression level among transfected U937 cells. A schematic illustration of the experimental outline is shown in supplementary material Fig. S1A–C. After metabolic labelling with different isotopes, equal numbers of cells were mixed, and subcellular fractions were subjected to SDS-PAGE followed by trypsin digestion (supplementary material Fig. S1A). Samples were processed as described in the Materials and Methods and we were able to identify and quantify a set of 890 differentially expressed proteins in the three subcellular fractions from endoglin transfectants (supplementary material Table S1). A summary of the top ten downregulated and upregulated proteins in both L-endoglin and S-endoglin transfectants is shown in supplementary material Table S2. Interestingly, many of these proteins (marked with an asterisk) were deregulated in both types of transfectants. The Venn diagram representation in Fig. 3 depicts the numbers of upregulated and downregulated proteins compared to values in mock transfectants. This representation shows that both endoglin

Journal of Cell Science (2014) 127, 2723–2735 doi:10.1242/jcs.143644

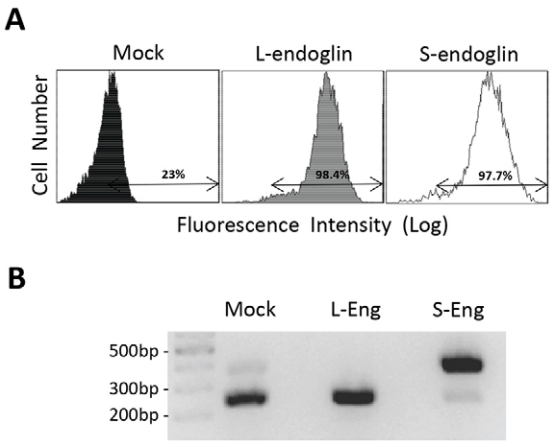

Fig. 2. Endoglin expression analysis in U937 transfectants. Stable U937 cell transfectants ectopically expressing L-endoglin (L-Eng), S-endoglin (S-Eng) as well as mock transfectants (Mock) were analysed by immunofluorescence flow cytometry with anti-endoglin antibodies (A); the percentage of positive cells is indicated by the horizontal bar. Semi-quantitative RT-PCR analysis shows the presence of L-endoglin and S-endoglin transcripts in transfectants (B).

isoforms produced the same effect in some of the regulated proteins, suggesting that this regulation is mediated by their shared extracellular domain (Fig. 3). In fact, the same regulatory effect was observed for 166 proteins (26 upregulated and 140 downregulated). By contrast, six proteins showed an opposite regulation between L-endoglin and S-endoglin transfectants (upregulated in L-endoglin and downregulated in S-endoglin cells). Of note, there were a large number of proteins (546) with a different behaviour in either L-endoglin (106 upregulated and 143 downregulated) or S-endoglin (36 upregulated and 261 downregulated) transfectants, suggesting that this effect depends on the endoglin cytoplasmic region.

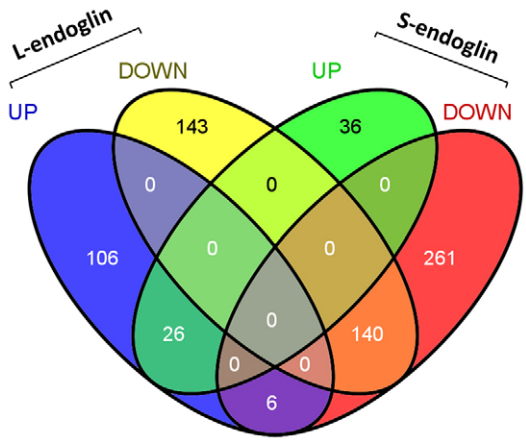

Fig. 3. Venn diagram representation of the protein identification summary of all subcellular fractions from L-endoglin and S-endoglin transfectants. Upregulated and downregulated protein levels are compared to values in mock transfectants. The same regulatory effect in both isoforms is observed for 166 proteins (26 upregulated and 140 downregulated). Six of the proteins show an opposite regulation between L-endoglin and S-endoglin transfectants (upregulated in L-endoglin and downregulated in S-endoglin cells). A large number of proteins (546) showed an regulation either by only L-endoglin (106 upregulated and 143 downregulated) or by only S-endoglin (36 upregulated and 261 downregulated) transfectants.

Validation studies and functional pathways analysis of the proteome list

To confirm the results from the SILAC analysis, we decided to validate some of the differentially expressed proteins. Nine representative proteins were selected for this purpose: Smad3, a transcription factor that mediates TGF-β signalling and whose activity is modulated by endoglin (Bernabeu et al., 2007); calmodulin, a Ca^{2+}-binding messenger protein that regulates inflammation, cell cycle, apoptosis and immune responses (Racioppi and Means, 2012); and CD13, a myeloid-specific cell surface alanyl aminopeptidase (Ansorge et al., 2009). In addition, superoxide dismutase 2 (SOD2), peroxiredoxin-1 (PRDX1), proline-serine-threonine phosphatase-interacting protein 1 (PSTPIP1), cyclin-dependent kinase 8 (CDK8), integrin α1 and cathepsin G were also selected. Among these, cathepsin G, PSTPIP1 and SOD2 are within the top three, top ten and top 16 dysregulated proteins, respectively (supplementary material Tables S1, S2). Analysis of the differentially expressed protein list showed that each of these proteins underwent a distinct regulation (supplementary material Table S1; Fig. 4A). Validation studies confirmed a similar behaviour by western blot and flow cytometry experiments (Fig. 4B). Thus, decreased protein levels of Smad3 and integrin α1 were detected in both endoglin transfectants, calmodulin and peroxiredoxin 1 protein levels did not change in L-endoglin transfectants, but were repressed in S-endoglin cells, and the protein expression of CD13, cathepsin G and PSTPIP1 was markedly increased in both endoglin transfectants compared with the mock condition.

Next, we investigated the possible biological functions affected by endoglin overexpression. The SILAC protein list was subjected to the bio-informatic Ingenuity pathways analysis (IPA) using the Ingenuity knowledge base (genes only) as a reference set. The top 25 significantly altered biofunctions are shown for L-endoglin and S-endoglin U937 transfectants with respect to mock controls in supplementary material Fig. S2. Among the cellular processes affected in both types of endoglin transfectants are cellular growth and proliferation, immune cell trafficking, cell death and survival, as well as homeostasis of free radicals, all of which are compromised during aging. To assess whether these cellular functions were indeed affected in endoglin transfectants, specific functional assays were carried out. Both endoglin transfectants show an altered 'cell trafficking' profile in the bioinformatics analysis, most likely due to the marked reduction of integrin levels, including those of the α1, α5, β1 and β2 subunits (Fig. 5A; supplementary material Table S1). Integrins are involved in cell adhesion, a process impaired during cellular senescence. Among the modulated integrins, integrin α5 is the one that showed the highest reduction ($\log_2$ ratios: L-endoglin, −0.827; S-endoglin, −0.881). Thus, we postulated that the decreased SILAC expression ratio of integrin α5 would lead to weaker cell adhesion to fibronectin. Indeed, cell adhesion assays clearly demonstrated an impaired binding of both endoglin transfectants to fibronectin compared to mock controls (Fig. 5B). Furthermore, the decreased cell adhesion could be observed at different adhesion time points (5–60 min). These data suggest that protein expression of both endoglin isoforms in monocytic cells reduces their adhesion to the extracellular matrix.

When cells enter senescence they undergo an arrest during the cell cycle and lose their capacity to proliferate. The IPA results

Journal of Cell Science (2014) 127, 2723–2735 doi:10.1242/jcs.143644

A

SILAC ratios of selected proteins

Protein	Long/Mock	Short/Mock
SOD2	2.799	…
PRDX1	…	0.725
PSTPIP1	3.204	2.397
SMAD3	0.606	0.740

Protein	Long/Mock	Short/Mock
CD13	1.651	1.659
CDK8	…	0.634
Calmodulin	…	0.794
Cathepsin-G	4.547	4.809
Integrin α1	0.697	0.741

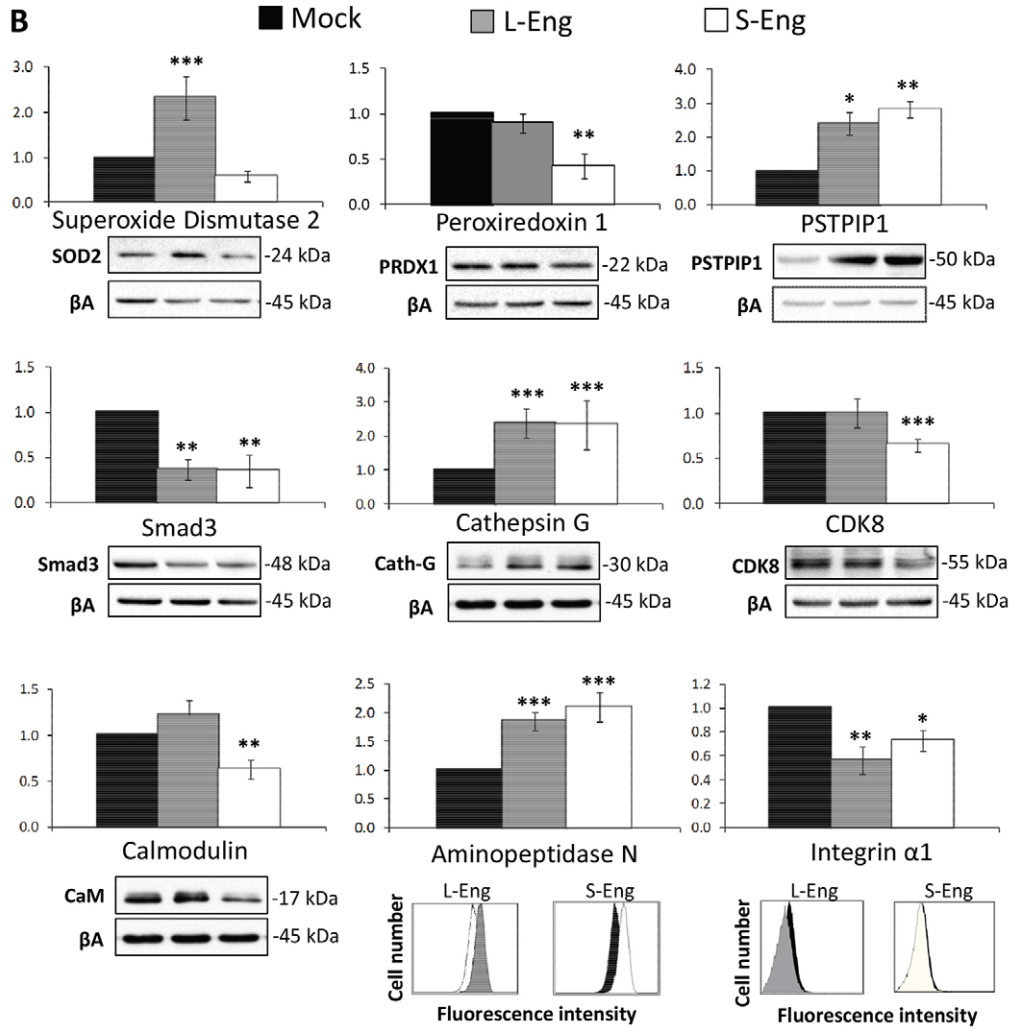

Fig. 4. Validation of SILAC analysis at individual protein level. (A) SILAC ratio obtained from the proteomic analysis of superoxide dismutase 2 (SOD2), peroxiredoxin 1, proline-serine-threonine phosphatase-interacting protein 1 (PSTPIP1), Smad3, cathepsin G (Cath-G), CDK8, calmodulin (CaM), aminopeptidase N (CD13) and integrin α1. The data has been adapted from supplementary material Table S1 and ratios are represented in a linear scale. Ratios within the 1.5–0.8 range are not included. (B) Western blot and immunofluorescence flow cytometry (bottom row) analyses of mock, S-endoglin (S-Eng) and L-endoglin (L-Eng) U937 transfectants using specific antibodies. Protein levels were quantified by densitometry of the specific bands relative to β-actin (βA) in western blot analyses and by measuring the expression index in flow cytometry analyses. Values are represented in the histograms where an arbitrary value of 1 is given to mock transfectants. The statistical significance with respect to mock cells is indicated. *$P<0.05$; **$P<0.01$; ***$P<0.001$.

also yielded ‘cell cycle’ as one of the compromised biological functions, although the statistical significance was much higher in S-endoglin (lowest *P*-value, 4.76×10^{-6}) than L-endoglin (lowest *P*-value, 3.99×10^{-4}) transfectants. This is in agreement with the decreased protein expression in S-endoglin, but not in L-endoglin, transfectants of cyclin-dependent kinases CDK1, CDK7 or CDK8, as well as in the cell cycle regulators cell division cycle 20 homolog (CDC20) and calmodulin (Fig. 5C; Fig. 4B). Indeed, the growth rate was significantly slower in S-endoglin transfectants compared to mock controls or L-endoglin transfectants (Fig. 5D). This retarded proliferation could be detected after 24 h of culture and was more evident 48 h after culture synchronization.

According to the IPA analysis, cell death and survival is affected in both the endoglin transfectants, although in opposite ways regarding apoptosis. Thus, pro-apoptotic proteins such as

Journal of Cell Science (2014) 127, 2723–2735 doi:10.1242/jcs.143644

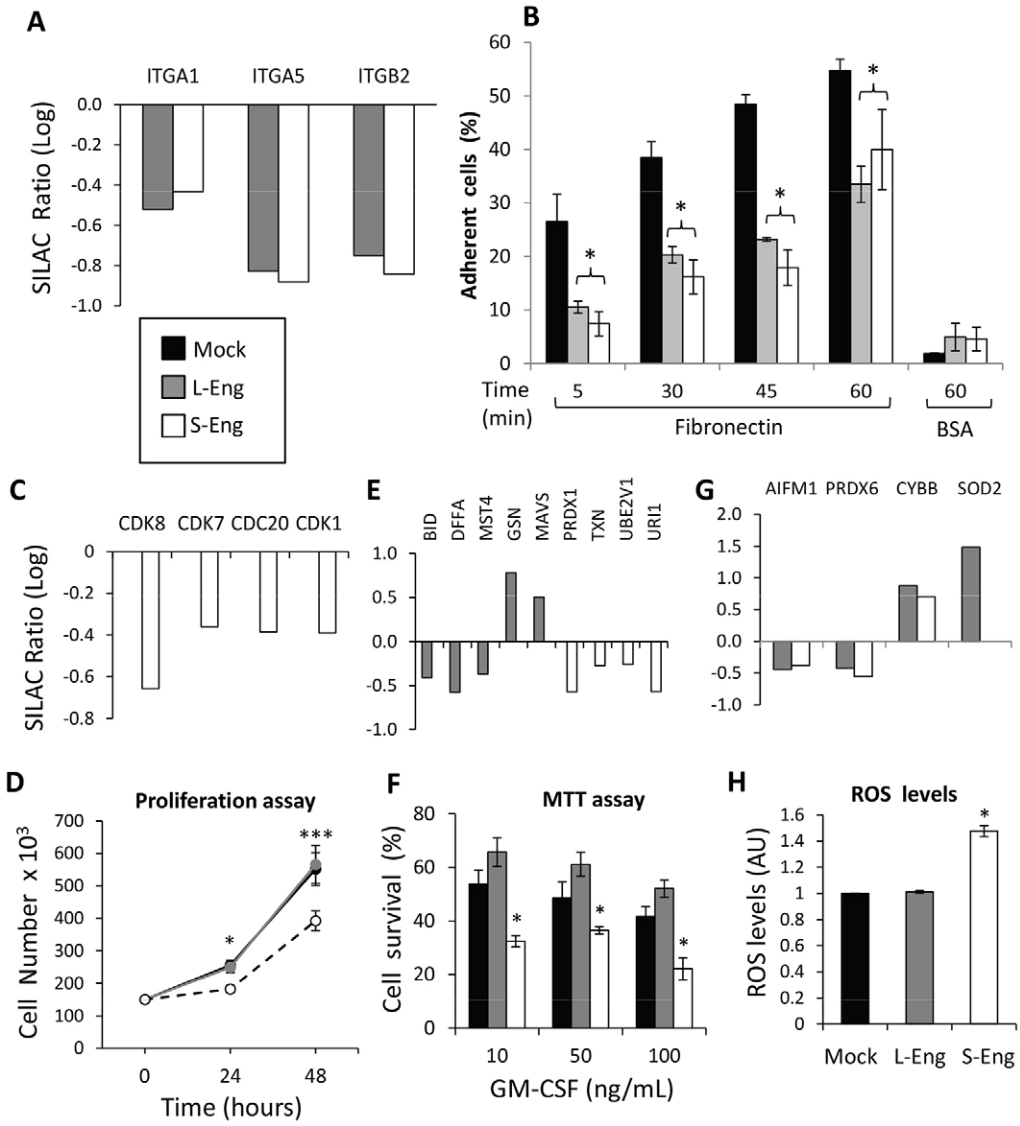

Fig. 5. Functional validation of the pathway analysis. (A,B) Integrin levels and cell adhesion. (A) SILAC ratio obtained from the proteomic analysis of β1 (*ITGA1*), α5 (*ITGA5*) and β2 (*ITGB2*) integrins (supplementary material Table S1) in a logarithmic scale. In both endoglin transfectants, these three integrin members showed a reduction in their expression levels, with α5 displaying the highest reduction (*ITGA5*; L-endoglin, −0.827 and S-endoglin, −0.881). (B) Cell adhesion to fibronectin. Plates were coated with fibronectin or BSA, as indicated. L-endoglin, S-endoglin and mock U937 transfectants were labelled with CFSE, loaded in the wells and incubated for different times. Each assay was performed in triplicate. The statistical significance of endoglin transfectants versus mock cells is indicated. *$P<0.05$. (C,D) Cell-cycle-related proteins and cellular proliferation. (C) SILAC ratio obtained from the proteomic analysis of cell-cycle-related proteins CDK8, CDK7, cell division cycle 20 homolog (CDC20) and CDK1 (supplementary material Table S1). (D) The proliferation rate of S-endoglin-overexpressing U937 cells is decreased compared to mock or L-endoglin transfectants. The differences are statistically significant at 24 h (255.67 in mock and 249.00 in L-endoglin versus 182.33 in S-endoglin; *$P<0.05$) and at 48 h (551.67 in mock and 566.00 in L-endoglin versus 392.33 in S-endoglin; ***$P<0.001$). (E,F) Cell survival, apoptosis and proteins involved. (E) SILAC ratio (log_2) obtained from the proteomic analysis of BH3-interacting domain death agonist (BID), DNA fragmentation factor subunit α (DFFA), mammalian STE20-like protein kinase 4 (MST4), gelsolin (GSN), mitochondrial antiviral signalling (MAVS), peroxiredoxin-1 (PRDX1), thioredoxin (TXN), ubiquitin-conjugating enzyme E2 variant 1 (UBE2V1) and unconventional prefoldin RPB5 interactor 1 (URI1), which are involved in cell survival and apoptosis (supplementary material Table S1). (F) U937 cells were treated with increasing concentrations of GM-CSF for 4 days and cell survival was determined using an MTT assay. (G,H) Reactive oxygen species and proteins involved. (G) SILAC ratio obtained from the proteomic analysis of apoptosis-inducing factor mitochondrion-associated 1 (AIFM1), peroxiredoxin-6 (PRDX6), cytochrome *b*-245 β (CYBB) and superoxide dismutase 2 (SOD2), which are involved in the homeostasis of free radicals (supplementary material Table S1). (H) U937 cells were incubated with the ROS indicator H_2DCFDA for 30 min in the dark at room temperature, lysed and their fluorescence was measured in a Varioskan Flash reader. Results are relative to mock transfectants (arbitrary value).

BH3-interacting domain death agonist (BID), DNA fragmentation factor subunit α (DFFA) or mammalian STE20-like protein kinase 4 (MST4) have lower expression in L-endoglin, but not in S-endoglin, transfectants, whereas pro-survival and apoptosis-protective proteins like gelsolin (GSN) or mitochondrial antiviral signalling (MAVS) have a higher expression in L-endoglin, but not S-endoglin, transfectants compared to mock controls (Fig. 5E). By contrast, in S-endoglin, but not in L-endoglin, transfectants, levels of pro-survival and anti-apoptosis proteins peroxiredoxin-1 (PRDX1), thioredoxin (TXN), ubiquitin-conjugating enzyme E2

variant 1 (UBE2V1) and unconventional prefoldin RPB5 interactor 1 (URI1) are reduced compared to mock controls. These data suggest that S-endoglin transfectants might exhibit a decreased survival in response to pro-apoptotic stimuli. To test this hypothesis, the granulocyte-macrophage colony-stimulating factor (GM-CSF)-induced pro-apoptotic effect in U937 cells (Okuma et al., 2000) was assessed. As shown in Fig. 5F, S-endoglin transfectants showed a decreased survival rate in response to three different doses of the pro-apoptotic cytokine, whereas L-endoglin transfectants showed a slightly higher, but not significant, survival rate than control cells.

The SILAC analysis also suggested that the metabolism of reactive oxygen species (ROS) was affected in both endoglin transfectants, as illustrated in Fig. 5G. Thus, the redox-homeostasis-maintaining protein apoptosis-inducing factor mitochondrion-associated 1 (AIFM1) and the antioxidant protein peroxiredoxin-6 (PRDX6) were downregulated, whereas the NADPH oxidase cytochrome *b*-245 β polypeptide (CYBB) was upregulated in endoglin transfectants. Based on these data, it can be postulated that L-endoglin and S-endoglin transfectants might display an enhanced production of ROS levels. However, this production might be compensated for in L-endoglin, but not in S-endoglin transfectants owing to increased protein levels of superoxide dismutase 2 (SOD2), which might contribute to free radical scavenging (Fig. 5G). This interpretation is compatible with the actual measurement of ROS production in U937 cells, showing that S-endoglin expressing cells display levels of ROS higher than those of L-endoglin or mock transfectants (Fig. 5H).

Overall, the selected proteins analysed in Fig. 5 represent a large number of proteins involved in immune cell trafficking, cellular growth and proliferation, and cell death and survival, as well as homeostasis of free radicals (supplementary material Fig. S2; Table S1). Given the high number of deregulated proteins involved in each of these biological processes, it is unclear what the specific contribution of each protein is. Rescue experiments of the biological functions might be useful to dissect the contribution of each protein. Taken together, these data suggest that protein expression of both endoglin isoforms affect the mentioned cellular processes associated with aging, whereas S-endoglin appears to contribute to cellular senescence.

Endoglin isoforms in macrophage polarization

It is well known that aging impairs macrophage polarization into M1 and M2 subtypes (Mahbub et al., 2012). Because S-endoglin is upregulated upon macrophage senescence *in vitro* and during *in vivo* aging (Fig. 1), we assessed the role of both endoglin isoforms in the phorbol myristate acetate (PMA)-induced macrophage differentiation of U937 cells (Cabañas et al., 1990). Thus, PMA-treated L-endoglin, S-endoglin and mock U937 transfectants were analysed by quantitative PCR to assess the transcript levels of different M1 and M2 marker genes (Fig. 6A). The expression of classical M1 interleukin genes, like *IL6*, *IL23A* or *IL12A*, was higher in mock and L-endoglin transfectants than in S-endoglin-transfected cells. By contrast, typical M2 genes, like musculoaponeurotic fibrosarcoma oncogene homolog B (*MAFB*), stabilin 1 (*STAB1*) or serpin peptidase inhibitor, clade B (*SERPINB2*) were more highly expressed in S-endoglin transfectants than in mock cells or L-endoglin transfectants (Fig. 6A). Therefore, and at the transcriptomic level, the presence of S-endoglin skews myeloid cell polarization towards M2, whereas the expression of L-endoglin does not have an overt influence of the gene expression of polarization markers, further emphasizing the different signalling capabilities of both endoglin isoforms.

Next, we assessed the potential influence of both endoglin isoforms on the functional polarization of myeloid cells using the PMA-induced differentiation of U937 cells. To that end, the responsiveness of endoglin transfectants to lipopolysaccharide (LPS), which favours the acquisition of an M1 phenotype, was evaluated (Fig. 6B). Analysis of the secreted cytokine profile showed the release of pro-inflammatory cytokines to the supernatant in mock, L-endoglin and S-endoglin populations (Fig. 6B). Overall, endoglin transfectants displayed lower levels of LPS-induced pro-inflammatory cytokines than mock controls (Fig. 6B). S-endoglin transfectants showed the lowest inflammatory response among the three cell types, in agreement with their M2-like phenotype observed in Fig. 6A. Moreover, L-endoglin cells displayed an inflammatory profile stronger than that of S-endoglin transfectants, a finding compatible with their gene expression pattern (Fig. 6A, upper panel). This M1-like phenotype associated with L-endoglin is especially evident in the case of the cytokines C5/C5a, I-309, IL8, IP10 and Rantes.

Next, we investigated the underlying molecular basis for the role of endoglin in macrophage polarization. It is noteworthy that activin-A is a key regulator of macrophage polarization that promotes a proinflammatory phenotype and inhibits the acquisition of an anti-inflammatory status (Sierra-Filardi et al., 2011). Because gene expression experiments showed an altered regulation of activin-A (*INHBA*) transcription in endoglin transfectants (Fig. 6A), we assessed the possible deregulated protein expression of this cytokine in U937 transfectants. Of note, and for technical reasons, our SILAC protein analysis did not include the secreted proteome fraction of the transfectants and therefore, no data about activin-A protein expression was available. As shown in Fig. 6D, secretion of activin-A was markedly increased (more than twofold) in L-endoglin transfectants compared to mock controls. By contrast, activin-A levels in culture supernatants of S-endoglin transfectants were clearly reduced relative to controls. Taken together, the polarization studies suggest that, in monocytic cells, L-endoglin promotes an M1-like phenotype, whereas S-endoglin favours the expression of M2 markers and functions.

DISCUSSION

The effect of aging on the innate immune system has a detrimental effect on the health of elderly individuals. Indeed, there is a substantial decline in the ability to resist infectious diseases and in the generation of robust protective immune responses among the elderly (Bender, 2003; Dace and Apte, 2008). Macrophages are crucial components of the innate immune system, but their senescence protein markers and related functions during aging have been poorly investigated. Here, we have analysed, for the first time, the regulated expression and function of two endoglin isoforms during macrophage senescence. We find that S-endoglin is a marker of macrophage senescence, being upregulated during *in vitro* senescence induced by oxidative stress and *in vivo* aging. This upregulation preceded that of PAI-1, a well-known senescence marker, suggesting that S-endoglin is an early marker of macrophage senescence. Previous studies have also shown that S-endoglin is a contributor to age-dependent cardiovascular pathology (Blanco et al., 2008). The upregulation of S-endoglin unbalances the ratio of S-endoglin to L-endoglin isoforms, in turn affecting the TGF-β signalling pathways of endothelial cells.

Journal of Cell Science (2014) 127, 2723–2735 doi:10.1242/jcs.143644

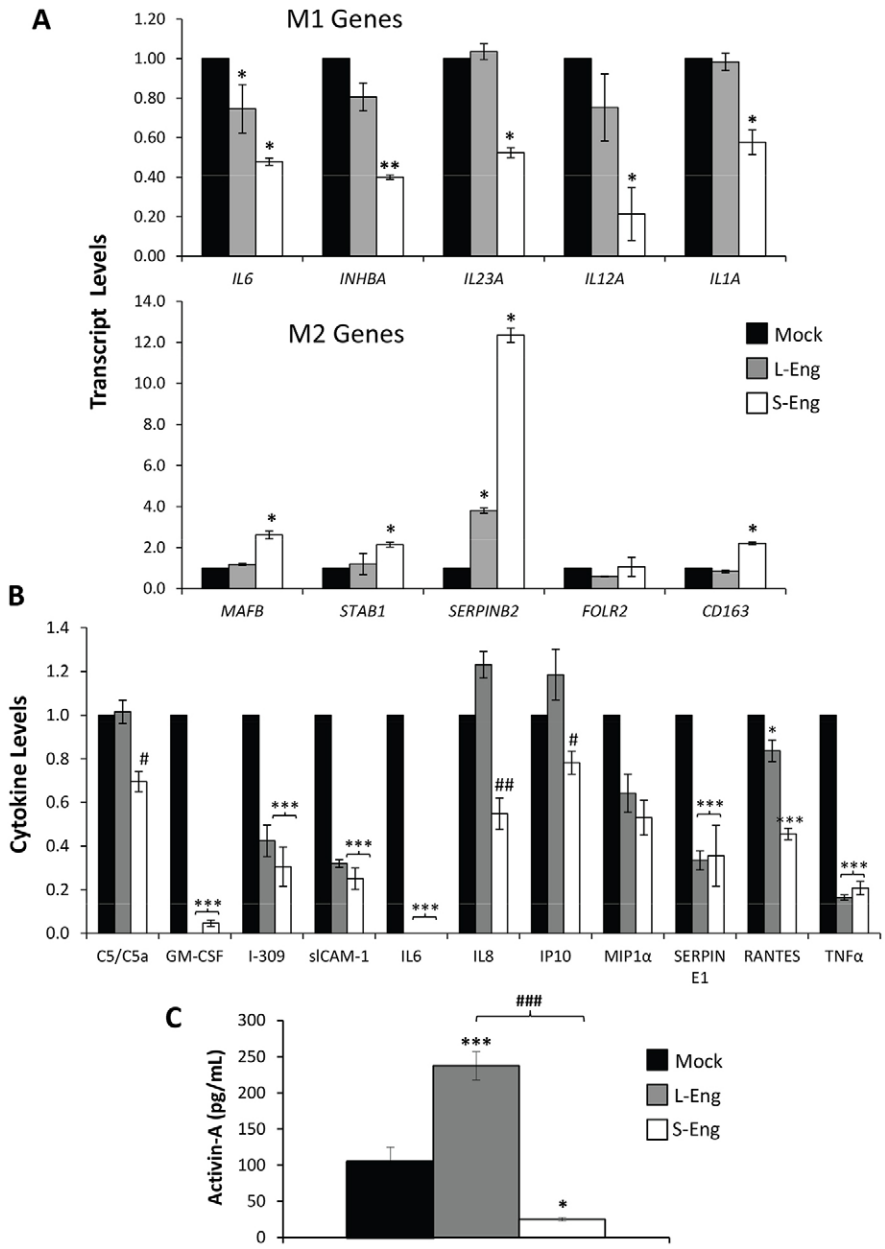

Fig. 6. Polarization of endoglin U937 transfectants. (A) Analysis of the M1 and M2 gene profile upon macrophage differentiation. Mock, L-endoglin and S-endoglin U937 transfectants were treated with PMA for 3 days and specific M1 (*IL6*, *INHBA*, *IL23A*, *IL2A* and *IL1A*) and M2 (*MAFB*, *STAB1*, *SERPINB2*, *FOLR2* and *CD163*) marker genes were analysed by quantitative RT-PCR. Results were normalized to the values for mock transfectants. L-endoglin and S-endoglin transfectants show an M1-like and M2-like phenotype, respectively. (B) U937 transfectants were treated with PMA, and LPS was added for the last 12 h of incubation. Inflammatory cytokines in the culture medium were analysed with a kit of capture antibodies spotted on nitrocellulose membranes. Expression of both endoglin isoforms impairs the typical inflammatory response compared to mock cells, although the overall inhibitory effect of S-endoglin was stronger than that of L-endoglin. Cytokine levels in the absence of stimuli were negligible. (C) Levels of activin-A in culture supernatants from mock, L-endoglin and S-endoglin transfectants were determined by ELISA. L-endoglin transfectants induce, whereas S-endoglin transfectants inhibit, the expression of activin-A. The statistical significance of endoglin transfectants versus mock cells (*$P<0.05$; **$P<0.01$; ***$P<0.001$) and of S-endoglin transfectants versus L-endoglin transfectants ($^{\#}P<0.05$; $^{\#\#}P<0.01$; $^{\#\#\#}P<0.001$) is indicated.

Both endoglin isoforms interact with the TGF-β signalling receptors types I (ALK1 and ALK5) and II (TβRII) and modulate cellular responses to TGF-β (Lastres et al., 1996; Guerrero-Esteo et al., 2002; Blanco et al., 2008; Velasco et al., 2008). More specifically, S-endoglin promotes the TGF-β–ALK5-dependent route, whereas L-endoglin activates the TGF-β–ALK1-dependent pathway. Interestingly, PAI-1 is a target gene of the S-endoglin–ALK5 pathway, suggesting that S-endoglin is upstream of PAI-1. This is in agreement with the upregulation of S-endoglin and PAI-1 in LPMs, but not in SPMs, and with the finding that the S-endoglin increase precedes that of PAI-1 in senescent macrophages.

To date, most of the studies on endoglin have been focused on the predominant L-endoglin isoform, although substantial levels of S-endoglin mRNA are coexpressed with L-endoglin *in vivo* (Bellón et al., 1993; Pérez-Gómez et al., 2005; Blanco et al.,

2008). Unfortunately, little is known about the role of endoglin isoforms in the myeloid lineage. To assess the impact of the two endoglin isoforms in monocytic cells, stable transfectants of U937 cells overexpressing human L-endoglin or S-endoglin were subjected to a proteomic analysis using the SILAC technology. The biological functions affected by endoglin overexpression were studied using IPA. This showed that, among the altered biofunctions, there were cellular processes affected in both types of endoglin transfectants, including cellular growth and proliferation, immune cell trafficking, and cell death and survival, as well as homeostasis of free radicals, all of which are compromised during aging. A common feature of L-endoglin and S-endoglin transfectants is their general decrease of integrin levels (at least α1, α5, β1 and β2 integrin subunits), in agreement with their decreased fibronectin-dependent cell adhesion. These data not only show that expression of both endoglin isoforms in monocytic cells reduces their adhesion to the extracellular matrix, but that it also impairs their trafficking, which necessarily involves cell adhesion. Supporting this interpretation, studies in different cell types have shown that overexpression of either L-endoglin or S-endoglin leads to reduced cellular migration (Guerrero-Esteo et al., 1999; Liu et al., 2002; Conley et al., 2004; Bernabeu et al., 2007). Furthermore, the upregulation of S-endoglin during macrophage senescence is in line with the decreased migration of myeloid cells, as well as the impaired anti-inflammatory response, observed during aging (Shaw et al., 2010; Li, 2013). Endoglin expression is finely regulated during hematopoietic development and differentiation. For example, hematopoietic stem cells express endoglin prior to a downregulation during cell development and mobilization (Chen et al., 2003). In addition, endoglin is markedly upregulated during monocyte activation to macrophages (Lastres et al., 1992). Thus, it can be postulated that the increased expression of endoglin is associated with resident niches of hematopoietic stem cells or tissue macrophages. Accordingly, the resident large macrophages of the peritoneal cavity are mostly senescent (Cassado Ados et al., 2011) and show increased endoglin expression during aging (Fig. 1E).

The shared behaviour of L-endoglin and S-endoglin U937 transfectants regarding integrin expression and cell adhesion can probably be explained by the fact that the extracellular domain of endoglin is the same in both isoforms. By contrast, other cellular functions were differentially affected by L-endoglin or S-endoglin expression, suggesting that these functions are dependent on the distinct cytoplasmic tail of each endoglin isoform. Thus, and at variance with L-endoglin, S-endoglin expression led to decreased cellular proliferation and a decreased survival response to GM-CSF-induced apoptosis, as well as to increased oxidative stress (Fig. 5). This phenotype of S-endoglin-expressing cells fits well with that of cellular senescence, suggesting that S-endoglin is not only a marker of macrophage senescence but also contributes to the compromised status of macrophage functions during aging (Allen, 1998; Colantoni et al., 2001; Lloberas and Celada, 2002; Plowden et al., 2004).

We also describe for the first time that endoglin expression alters the differentiation and polarization processes of macrophages (Fig. 6). Polarization of macrophages is crucial in the immune response to pathogens, and in tumour progression, autoimmunity and fibrosis (Werner and Alzheimer, 2006; Benoit et al., 2008); this polarization activity is impaired during aging, leading to a deficient macrophage function and activation (Gomez et al., 2005; Pello et al., 2011). Macrophages can be subdivided into classical pro-inflammatory M1 macrophages, or alternative anti-inflammatory M2 macrophages (Mantovani et al., 2004). Importantly, these macrophage subpopulations are capable of switching phenotypes based on the stimuli (Arnold et al., 2007). Our polarization studies suggest that in monocytic U937 cells, L-endoglin promotes an M1-like phenotype, whereas S-endoglin favours the expression of M2 markers (Fig. 6). Classically activated M1 macrophages secrete pro-inflammatory cytokines, such as tumor necrosis factor (TNF-α), interleukin-12 (IL-12) and the TGF-β family member activin-A, and exert anti-tumoricidal activity. By contrast, activated M2 macrophages secrete anti-inflammatory cytokines, such as IL-4, IL-10 and TGF-β1, which promote age-associated processes, such as fibrosis, atherosclerosis and tumour growth (Mantovani et al., 2004; Pello et al., 2011). These findings suggest that S-endoglin might contribute to the abnormal inflammatory response associated with aging by inducing an M2-like phenotype in macrophages.

The opposing behaviour of L-endoglin versus S-endoglin regarding the M1–M2 polarization is clearly illustrated by the basal secretion of activin-A in U937 transfectants (Fig. 6D). Activin-A expression is upregulated on activation and in response to inflammatory mediators (Jones et al., 2007; Robson et al., 2008; Phillips et al., 2009), but is suppressed by anti-inflammatory glucocorticoids (Yu et al., 1996; Scutera et al., 2008). We find that production of activin-A is markedly increased by L-endoglin and clearly reduced by S-endoglin, in agreement with the M1-like and M2-like phenotypes, respectively. Of note, activin-A is a key modulator of the polarization (Sozzani and Musso, 2011), whose activity depends on the species and environmental context. Recently, it has been described that activin-A contributes to M1 macrophage polarization and prevents the expression of M2-specific markers in humans (Sierra-Filardi et al., 2011) Interestingly, a steep increase in activin-A levels during aging, especially in the last decades of life has been described in healthy adult men and post-menopausal women (Baccarelli et al., 2001). Because activin-A is a ligand of endoglin (Barbara et al., 1999), the functional interplay between the S-endoglin and activin-A in senescent macrophages deserves to be further investigated.

MATERIALS AND METHODS

Cell culture and SILAC

Stable transfectants of endoglin isoforms (L and S) and mock condition (M) in the U937 cell line were cultured as described previously (Lastres et al., 1996). For the SILAC assays, cells were cultured in specific SILAC-ready RPMI 1640 (Thermo Scientific) supplemented with 10% dialysed fetal bovine serum, 100 U/ml streptomycin/penicillin at 37℃ under a humidified atmosphere with 5% CO_2. Metabolic labelling of transfectants with non-radioactive isotopes was carried out as follows: (1) Light-isotope labelling, L-Lys + L-Arg; (2) medium-isotope labelling, [$^{13}C_6$]L-Lys + [$^{13}C_6$]L-Arg; and (3) heavy-isotope labelling, [$^{13}C_6$],[$^{15}N_2$]L-Lys + [$^{13}C_6$],[$^{15}N_4$]L-Arg (Thermo Scientific). Cell viability was checked by Trypan Blue staining and proliferation was measured in a Neubauer chamber. At a population doubling level of six (a label up to 95% is assumed), equal numbers of cells were mixed in the direct combination ($Mock_{Light}$+L-Eng_{Heavy}+S-Eng_{Medium}) and swapping ($Mock_{Medium}$+L-Eng_{Light}+S-Eng_{Heavy}). Then, protein enrichment was made after subcellular fractioning into membrane, cytoplasmic and nuclear compartments, using the subcellular protein fractionation kit for cells in culture (Thermo Scientific). Fractions were individually loaded and separated in non-reducing and queratin-free SDS-PAGE. After staining with colloidal Coomassie (Invitrogen), the entire gel lane was cut into 10–14 pieces of equal size and subjected to in-gel tryptic digestion

essentially as described previously (Wilm et al., 1996). Briefly, the gel pieces were destained and washed and, after dithiothreitol reduction and iodoacetamide alkylation, proteins were digested with porcine trypsin (sequencing grade modified; Promega, Madison, WI) overnight at 37℃. The resulting tryptic peptides were extracted from the gel pieces with 30% acetonitrile and 0.3% trifluoroacetic acid, and the mixture was evaporated in a vacuum centrifuge to remove the organic solvents. For validation studies, U937 cell transfectants were grown in standard RPMI medium supplemented with 10% heat-inactivated fetal calf serum (FCS), 2 mM L-glutamine, and 100 U/ml penicillin/streptomycin.

Protein mass spectrometry analysis

Briefly, peptides were loaded onto a C18-A1 ASY-Column 2-cm precolumn (Thermo Scientific) and then eluted onto a Biosphere C18 column (NanoSeparations) and separated using a 180-min gradient [170 min with 2–35% acetonitrile (ACN) gradient using buffer A, 0.1% formic acid, 2% ACN; and buffer B, 0.1% formic acid, 99.9% ACN] at a flow-rate of 250 nl/min on a nanoEasy HPLC (Proxeon) coupled to a nanoelectrospray ion source (Proxeon). Mass spectra were acquired on the LTQ-Orbitrap Velos (Thermo Scientific) in the positive ion mode. Singly charged ions and unassigned charge states were rejected. After mass spectrometry analysis, raw files were searched against the human SwissProt database (SwissProt_57.15.fasta) using the MASCOT search engine (version 2.3, Matrix Science) through Proteome Discoverer (version 1.3.0.339) (Thermo). Identified peptides were validated using Percolator algorithm (Käll et al., 2007) with a q-value threshold of 0.01, and their relative quantification was performed using Proteome Discoverer software. Light, medium and heavy spectra of the peptides were analysed to get the protein level ratios based on the detected relative abundance (supplementary material Fig. S1B). The final list of differentially expressed proteins was obtained by correcting the ratio deviation among samples. Thus, a truncated mean (or trimmed mean) was applied to initially obtained ratios (supplementary material Fig. S1C). In addition, individual peptide analysis using the Proteome Discoverer software was carried out to correct for the weak, but significant, arginine to proline metabolic switch (data not shown). For each SILAC triplet (light, medium and heavy), Proteome Discoverer determines the area of the extracted ion chromatogram and computes the ratios of different combinations – heavy:light and medium:light (direct) and light:medium and heavy:medium (swapping). Protein ratios are then calculated as the median of all the quantified unique peptides belonging to a certain protein. The final list was manually filtered excluding proteins between 1.5 and 0.8 ratio and/or with different values or poor peptide resolution in direct or swapping experiments. Values are presented and analysed as the $\log_2$ of the obtained average ratio of direct:swapping (L-Eng:Mock and S-Eng:Mock). The logarithmic ratio distribution of the SILAC raw data after normalization respect to mock transfectants is shown in supplementary material Fig. S3. As expected, most of the identified proteins for both transfectants (>4000) have a value around zero (no change compared to Mock). The definitive protein list with the average of ratios was analysed using IPA software (Ingenuity Systems). The protein list was clustered on a Venn diagram in order to identify proteins that were either significantly up or down expressed in both L-endoglin and S-endoglin transfectants compared to controls. The image was obtained by an online tool developed in the Centro Nacional de Biotecnología (CNB, CSIC, Madrid) (Oliveros et al., 2000).

Immunodetection assays

For western blot analysis, transfectant cells were lysed in lysis buffer (10 mM Tris-HCl pH 8, 150 mM NaCl, 1% NP-40, and a cocktail of protease and phosphatase inhibitors) at 4℃. Lysate aliquots containing 40 µg protein were separated by SDS-PAGE under non-reducing conditions. After separation, samples were electrotransferred onto a PVDF membrane using the iBlot® System (Invitrogen). Immunodetection was carried out by probing the membrane with rabbit polyclonal antibodies against Smad3 (sc-6202), calmodulin (sc-5537), cathepsin-G (sc-6512), CDK8 (sc-1521), PRX1 (sc-7381), PSTPIP1 (sc-390727) (all Santa Cruz Biotechnology) or superoxide dismutase (S5069, Sigma) overnight at 4℃, using a mouse monoclonal anti-β-actin antibody (AC-15, Sigma) as a loading control, followed by incubation with the corresponding horseradish-peroxidase-conjugated secondary antibody. Protein bands were revealed using the SuperSignal chemiluminescent substrate (Pierce, Rockford, IL, USA) and quantified using the Molecular Imager® Gel Doc™ XR+ System with Image Lab™ Software. For immunofluorescence flow cytometry, cells were collected, centrifuged and washed twice with 4℃ PBS. After blocking with 2% human AB^+ serum in PBS for 30 min, cells were incubated with the mouse monoclonal anti-endoglin (P4A4; Developmental Studies Hybridoma Bank, University of Iowa), anti-CD13 (sc-53970, Santa Cruz Biotechnology) or anti-α1 integrin (TS2/7; Francisco Sanchez-Madrid, Hospital de La Princesa, Madrid, Spain) antibodies, followed by incubation with Alexa-Fluor-488-conjugated goat anti-mouse-Ig antibody (Invitrogen). Samples were analysed in an EPICS Coulter XL flow cytometer. Results are expressed as an expression index, calculated as the percentage of positive cells multiplied by their mean fluorescence intensity. For activin-A measurements, culture supernatants from U937 cells were collected and centrifuged at 3000 ***g*** for 10 min to pellet cellular debris. The levels of activin-A in the supernatants were determined using the human Activin-A Quantikine ELISA kit (ARY005; R&D Systems), following the manufacturer's instructions.

Proliferation, survival and apoptosis assays

For proliferation assays, U937 cells were cultured at 1.2×10^5 cells/ml in RPMI 1640 medium supplemented with 10% FCS and growth was observed at 24, 48 and 72 h. Proliferation measurements were carried out by cell counting after Trypan Blue staining in a Neubauer chamber or in a TC10 automated cell counter (BioRad). Each measurement was performed in triplicate. For survival assays, U937 cells were seeded at 4×10^4–8×10^4 cells/ml in a 96-well plate and induction of apoptosis was carried out by culturing the cells in the presence or absence of GM-CSF cytokine (10, 50 and 100 ng/ml) for up 4 days. Cultured cells were harvested and incubated with MTT (0.25 µg/µl; Sigma) at 37℃ under 5% CO_2 for 2 h. Then, the plate was centrifuged at 100 ***g*** for 10 min and, after discarding the medium, precipitated formazan crystals, generated by a differential activity of succinate dehydrogenase, were resuspended in DMSO. The absorbance was measured at 595 nm, followed by a background subtraction at 630 nm, in an IEMS Reader (Thermo Scientific).

Measurement of ROS

For detection of ROS, U937 cells were incubated in 10 µM 2′,7′-dichlorodihydrofluorescein diacetate (H_2DCFDA) (Invitrogen, Paisley, UK) for 30 min at room temperature in the dark. Samples were washed twice and finally resuspended in NaOH 0.25 M to determine the intracellular ROS levels. Fluorescence in lysates was measured in a Varioskan Flash spectral scanning multimode reader (Thermo Scientific). The relative fluorescence was normalized to the total protein content in each condition. The protein concentration was determined by the bicinchoninic acid assay (BCA protein assay kit, Pierce, Rockford, IL, USA) using BSA as standard and following the manufacturer's instructions.

Cell adhesion assay to fibronectin

For cellular adhesion to fibronectin-coated surfaces, 24-well plates were coated with 1 µg/cm^2 of human fibronectin in 500 µl (Sigma) at 37℃ for 1 h. A total of 500,000 cells were washed twice in PBS, labelled with the fluorescence probe carboxyfluorescein diacetate, succinimidyl ester (CFSE, Invitrogen) and assayed. After the indicated time, cells attached to the wells were washed and then lysed (25 mM Tris-phosphate pH 7.8, 2 mM DTT, 2 mM CDTA, 10% glycerol, 1% Triton X-100). Fluorescence in lysates was measured in a Varioskan Flash spectral scanning multimode reader (Thermo Scientific).

Oxidative-stress-induced senescence in human and mouse macrophages

Buffy coats were obtained from the Centro de *Transfusion de la Comunidad de Madrid*, after informed consent and according to

institutional guidelines. Human monocytes from four different donors were purified from peripheral blood mononuclear cells (PBMCs) by magnetic cell sorting using CD14 Microbeads (Miltenyi Biotec). Monocytes (≥95% $CD14^+$ cells) were cultured at 0.5×10^6 cells/ml for three days in RPMI medium supplemented with 10% FCS (complete medium) at 37℃ under a humidified atmosphere with 5% CO_2. Resident LPMs were isolated from mice as described below and then were incubated in complete medium for 2 h at 37℃ under 5% CO_2. Then, the medium was removed and plates were washed with PBS to eliminate cells in suspension and enrich for adherent cells. After adherence, the typical change in morphology was observed in human and mouse macrophages. To induce oxidative stress, H_2O_2 at 150 µM was added for 1 h, then the cells were washed twice with PBS and cultured for an additional 12 h in normal fresh medium. Cellular senescence was monitored by senescence-associated β-galactosidase activity (SA-β-Gal), as previously described (Haendeler et al., 2004; Blanco et al., 2008; Cassado Ados et al., 2011).

Macrophage differentiation and polarization of U937 cells

Stable U937 transfectants were cultured at 2×10^5 cells/ml for three days in complete RPMI with or without 50 nM phorbol-12-myristate-13-acetate (PMA). Upon treatment with PMA, cells underwent growth arrest and a change of morphology owing to their attachment to the substrate. The differentiation to macrophages was confirmed using immunofluorescence flow cytometry by measuring the increased surface expression of CD11b (Bear-1 antibody; ab36939, Abcam). For polarization studies, U937 stable transfectants were differentiated to macrophages with PMA as above, but adding 25 µg/ml of LPS for the last 12 h of PMA treatment. The amount of the cytokines present in the supernatant after the LPS/PMA treatment was analysed with the Human Cytokine Array panel A (R&D Systems), according to the manufacturer's instructions.

Animals

Specified pathogen-free C57Bl/6J male 8–48-week-old mice were used in the experiments. All animal procedures were in accordance with the guidelines for animal use published by Conseil de l'Europe (No. L358/1-358/6, 1986), Spanish Government (BOE No. 67, pp. 8509–8512, 1988, and BOE No. 256, pp. 31349–31362, 1990) and were approved by the National Research Council of Spain (CSIC) Animal Care and Use Committee. In order to recruit SPMs, mice were intraperitoneally injected with 1 mg of Zymosan A from *Saccharomyces cerevisiae* (Z4250, Sigma-Aldrich) in 0.5 ml of sterile PBS. For the isolation of peritoneal cavity cells (both recruited SPMs and tissue-resident LPMs) all animals were deeply anaesthetized with isofluorane and killed by cervical dislocation. After injecting 10 ml of sterile PBS into the peritoneal cavity, a massage was performed for a few seconds and ~8–9 ml of the injected liquid was recovered. Then, always under sterile conditions, the cell suspension was transferred to a 15-ml tube and centrifuged at 250 ***g*** for 6 min. The pellet was resuspended in 1 ml DMEM with 10% FCS, and the cell suspension was divided in wells of a P-6 plate and brought to a final volume of 2.5 ml of DMEM with 10% FCS. Cells were incubated for 2 h at 37℃ under 5% CO_2. After this time, the medium was removed and washed with 3 ml of PBS to remove the suspended cells and enrich the sample with adherent cells (macrophages from the peritoneal cavity). The cells were maintained in culture in DMEM with 10% FCS and the medium was changed every 24 h.

Quantitative real-time RT-PCR

Total RNA was isolated from cells using the SpeedTools total RNA extraction kit (Biotools) and reverse-transcribed using iScript cDNA Synthesis kit (BioRad). The cDNA was amplified in triplicates using specific oligonucleotides. For experiments with U937 cells, oligonucleotides for selected genes were designed according to the Universal Probe Library System (Roche Diagnostics) for quantitative real-time PCR (qRT-PCR). For the U937 polarization and phenotype screening, the levels of typical M1 or M2 genes were normalized to those of the TBP (TATA box binding protein), HPRT1 (hypoxanthine phosphoribosyltransferase 1) and RPLPO (large ribosomal protein) housekeeping genes. For experiments with human and mouse macrophages, the cDNA was used as a template for real-time PCR performed with specific primers. Mouse primers were: Pai1 (FW, 5′-GTCTTTCCGACCAAGAGCAG-3′; RV, 5′-GACAAAGGCT-GTGGAGGAAG-3′); S-endoglin and L-endoglin (FW, 5′-GACCTGTCT-GGTAAAGGCCTTGTCCTG-3′); L-endoglin (RV, 5′-CTGGGGCCAC-GTGTGTGAGAATAG-3′); S-endoglin (RV, 5′-CTGAGGGGCGTGGG-TGAAGG-3′). Human primers were: PAI1 (FW, 5′-CAGACCAAGAGC-CTCTCCAC-3′; RV, 5′-ATCACTTGGCCCATGAAAAG-3′); L-endoglin and S-endoglin (FW, 5′-ACCTGTCTGGTTGCACAAGCAAAGG-3′); L-endoglin (RV, GGGAACCGCGTGTGCGAGTAG-3′); S-endoglin (RV-5′-GGGAACCTGGGAGCGGGG-3′). Primers for human and mouse 18S rRNA were: FW, 5′-CTCAACACGGGAAACCTCAC-3′; and RV, 5′-CGCTCCACCAACTAAGAACG-3′. Samples were amplified using the iQ SyBR-Green Supermix (BioRad). Amplicons were detected using an iQ5 real-time detection system (BioRad). Transcript levels were normalized to 18S levels.

Statistical analysis

All the experiments were performed at least three times. Statistical analyses were performed on GraphPad Prism 5 for Windows (La Jolla, CA). All the statistical data are presented as mean±s.d. Statistical significance was calculated using an unpaired, two-tailed Student's *t* test or, when appropriate, by ANOVA followed by Bonferroni's post hoc testing. A value of $P<0.05$ was considered significant.

Acknowledgements

We thank Maria F. Lopez-Lucendo and Carmen Langa for excellent technical assistance and Jose I. Casal for helpful comments on the SILAC method (all Centro de Investigaciones Biologicas, CSIC, Madrid, Spain).

Competing interests

The authors declare no competing interests.

Author contributions

Experiments were performed by M.A., F.J.B., M.d.L.C.-E., L.O.-F. and E.G.-V. The manuscript was written by M.A. and C.B. L.M.B. and A.C. assisted in evaluating macrophage results. The study was designed and jointly supervised by C.B. and F.J.B.

Funding

This study was supported by grants from Ministerio de Economia y Competitividad of Spain [grant number SAF2010-19222 to C.B.]; and Centro de Investigación Biomédica en Red de Enfermedades Raras (CIBERER) (to C.B.). CIBERER is an initiative of the Instituto de Salud Carlos III (ISCIII) of Spain supported by FEDER funds. M.A. was supported by a fellowship from Ministerio de Ciencia e Innovación [grant number BES-2008-003888].

Supplementary material

Supplementary material available online at
http://jcs.biologists.org/lookup/suppl/doi:10.1242/jcs.143644/-/DC1

References

Allen, R. G. (1998). Oxidative stress and superoxide dismutase in development, aging and gene regulation. *Age (Omaha)* **21**, 47-76.

Alt, A., Miguel-Romero, L., Donderis, J., Aristorena, M., Blanco, F. J., Round, A., Rubio, V., Bernabeu, C. and Marina, A. (2012). Structural and functional insights into endoglin ligand recognition and binding. *PLoS ONE* **7**, e29948.

Ansorge, S., Bank, U., Heimburg, A., Helmuth, M., Koch, G., Tadje, J., Lendeckel, U., Wolke, C., Neubert, K., Faust, J. et al. (2009). Recent insights into the role of dipeptidyl aminopeptidase IV (DPIV) and aminopeptidase N (APN) families in immune functions. *Clin. Chem. Lab. Med.* **47**, 253-261.

Arnold, L., Henry, A., Poron, F., Baba-Amer, Y., van Rooijen, N., Plonquet, A., Gherardi, R. K. and Chazaud, B. (2007). Inflammatory monocytes recruited after skeletal muscle injury switch into antiinflammatory macrophages to support myogenesis. *J. Exp. Med.* **204**, 1057-1069.

Baccarelli, A., Morpurgo, P. S., Corsi, A., Vaghi, I., Fanelli, M., Cremonesi, G., Vaninetti, S., Beck-Peccoz, P. and Spada, A. (2001). Activin A serum levels and aging of the pituitary-gonadal axis: a cross-sectional study in middle-aged and elderly healthy subjects. *Exp. Gerontol.* **36**, 1403-1412.

Barbara, N. P., Wrana, J. L. and Letarte, M. (1999). Endoglin is an accessory protein that interacts with the signaling receptor complex of multiple members of the transforming growth factor-beta superfamily. *J. Biol. Chem.* **274**, 584-594.

Bellón, T., Corbí, A., Lastres, P., Calés, C., Cebrián, M., Vera, S., Cheifetz, S., Massague, J., Letarte, M. and Bernabéu, C. (1993). Identification and expression of two forms of the human transforming growth factor-beta-binding protein endoglin with distinct cytoplasmic regions. *Eur. J. Immunol.* **23**, 2340-2345.

Bender, B. S. (2003). Infectious disease risk in the elderly. *Immunol. Allergy Clin. North Am.* **23**, 57-64.
Benoit, M., Desnues, B. and Mege, J. L. (2008). Macrophage polarization in bacterial infections. *J. Immunol.* **181**, 3733-3739.
Bernabeu, C., Conley, B. A. and Vary, C. P. (2007). Novel biochemical pathways of endoglin in vascular cell physiology. *J. Cell. Biochem.* **102**, 1375-1388.
Bernabeu, C., Lopez-Novoa, J. M. and Quintanilla, M. (2009). The emerging role of TGF-beta superfamily coreceptors in cancer. *Biochim. Biophys. Acta* **1792**, 954-973.
Blanco, F. J. and Bernabeu, C. (2011). Alternative splicing factor or splicing factor-2 plays a key role in intron retention of the endoglin gene during endothelial senescence. *Aging Cell* **10**, 896-907.
Blanco, F. J. and Bernabeu, C. (2012). The splicing factor SRSF1 as a marker for endothelial senescence. *Front. Physiol.* **3**, 54.
Blanco, F. J., Grande, M. T., Langa, C., Oujo, B., Velasco, S., Rodriguez-Barbero, A., Perez-Gomez, E., Quintanilla, M., López-Novoa, J. M. and Bernabeu, C. (2008). S-endoglin expression is induced in senescent endothelial cells and contributes to vascular pathology. *Circ. Res.* **103**, 1383-1392.
Borges, L., Iacovino, M., Mayerhofer, T., Koyano-Nakagawa, N., Baik, J., Garry, D. J., Kyba, M., Letarte, M. and Perlingeiro, R. C. (2012). A critical role for endoglin in the emergence of blood during embryonic development. *Blood* **119**, 5417-5428.
Cabañas, C., Sanchez-Madrid, F., Aller, P., Yague, E. and Bernabeu, C. (1990). Phorbol esters induce differentiation of U-937 human promonocytic cells in the absence of LFA-1/ICAM-1-mediated intercellular adhesion. *Eur. J. Biochem.* **191**, 599-604.
Cassado Ados, A., de Albuquerque, J. A., Sardinha, L. R., Buzzo, C. L., Faustino, L., Nascimento, R., Ghosn, E. E., Lima, M. R., Alvarez, J. M. and Bortoluci, K. R. (2011). Cellular renewal and improvement of local cell effector activity in peritoneal cavity in response to infectious stimuli. *PLoS ONE* **6**, e22141.
Castonguay, R., Werner, E. D., Matthews, R. G., Presman, E., Mulivor, A. W., Solban, N., Sako, D., Pearsall, R. S., Underwood, K. W., Seehra, J. et al. (2011). Soluble endoglin specifically binds bone morphogenetic proteins 9 and 10 via its orphan domain, inhibits blood vessel formation, and suppresses tumor growth. *J. Biol. Chem.* **286**, 30034-30046.
Cheifetz, S., Bellón, T., Calés, C., Vera, S., Bernabeu, C., Massagué, J. and Letarte, M. (1992). Endoglin is a component of the transforming growth factor-beta receptor system in human endothelial cells. *J. Biol. Chem.* **267**, 19027-19030.
Chen, C. Z., Li, L., Li, M. and Lodish, H. F. (2003). The endoglin(positive) sca-1(positive) rhodamine(low) phenotype defines a near-homogeneous population of long-term repopulating hematopoietic stem cells. *Immunity* **19**, 525-533.
Colantoni, A., Idilman, R., de Maria, N., Duffner, L. A., Van Thiel, D. H., Witte, P. L. and Kovacs, E. J. (2001). Evidence of oxidative injury during aging of the liver in a mouse model. *Journal of the American Aging Association* **24**, 51-57.
Conley, B. A., Smith, J. D., Guerrero-Esteo, M., Bernabeu, C. and Vary, C. P. (2000). Endoglin, a TGF-beta receptor-associated protein, is expressed by smooth muscle cells in human atherosclerotic plaques. *Atherosclerosis* **153**, 323-335.
Conley, B. A., Koleva, R., Smith, J. D., Kacer, D., Zhang, D., Bernabéu, C. and Vary, C. P. (2004). Endoglin controls cell migration and composition of focal adhesions: function of the cytosolic domain. *J. Biol. Chem.* **279**, 27440-27449.
Dace, D. S. and Apte, R. S. (2008). Effect of senescence on macrophage polarization and angiogenesis. *Rejuvenation Res.* **11**, 177-185.
Ghosn, E. E., Cassado, A. A., Govoni, G. R., Fukuhara, T., Yang, Y., Monack, D. M., Bortoluci, K. R., Almeida, S. R., Herzenberg, L. A. and Herzenberg, L. A. (2010). Two physically, functionally, and developmentally distinct peritoneal macrophage subsets. *Proc. Natl. Acad. Sci. USA* **107**, 2568-2573.
Gomez, C. R., Boehmer, E. D. and Kovacs, E. J. (2005). The aging innate immune system. *Curr. Opin. Immunol.* **17**, 457-462.
Guerrero-Esteo, M., Lastres, P., Letamendía, A., Pérez-Alvarez, M. J., Langa, C., López, L. A., Fabra, A., García-Pardo, A., Vera, S., Letarte, M. et al. (1999). Endoglin overexpression modulates cellular morphology, migration, and adhesion of mouse fibroblasts. *Eur. J. Cell Biol.* **78**, 614-623.
Guerrero-Esteo, M., Sanchez-Elsner, T., Letamendia, A. and Bernabeu, C. (2002). Extracellular and cytoplasmic domains of endoglin interact with the transforming growth factor-beta receptors I and II. *J. Biol. Chem.* **277**, 29197-29209.
Haendeler, J., Hoffmann, J., Diehl, J. F., Vasa, M., Spyridopoulos, I., Zeiher, A. M. and Dimmeler, S. (2004). Antioxidants inhibit nuclear export of telomerase reverse transcriptase and delay replicative senescence of endothelial cells. *Circ. Res.* **94**, 768-775.
Jones, K. L., Mansell, A., Patella, S., Scott, B. J., Hedger, M. P., de Kretser, D. M. and Phillips, D. J. (2007). Activin A is a critical component of the inflammatory response, and its binding protein, follistatin, reduces mortality in endotoxemia. *Proc. Natl. Acad. Sci. USA* **104**, 16239-16244.
Käll, L., Canterbury, J. D., Weston, J., Noble, W. S. and MacCoss, M. J. (2007). Semi-supervised learning for peptide identification from shotgun proteomics datasets. *Nat. Methods* **4**, 923-925.
Kapur, N. K., Wilson, S., Yunis, A. A., Qiao, X., Mackey, E., Paruchuri, V., Baker, C., Aronovitz, M. J., Karumanchi, S. A., Letarte, M. et al. (2012). Reduced endoglin activity limits cardiac fibrosis and improves survival in heart failure. *Circulation* **125**, 2728-2738.
Koleva, R. I., Conley, B. A., Romero, D., Riley, K. S., Marto, J. A., Lux, A. and Vary, C. P. (2006). Endoglin structure and function: Determinants of endoglin phosphorylation by transforming growth factor-beta receptors. *J. Biol. Chem.* **281**, 25110-25123.
Lastres, P., Bellon, T., Cabañas, C., Sanchez-Madrid, F., Acevedo, A., Gougos, A., Letarte, M. and Bernabeu, C. (1992). Regulated expression on human macrophages of endoglin, an Arg-Gly-Asp-containing surface antigen. *Eur. J. Immunol.* **22**, 393-397.
Lastres, P., Martín-Perez, J., Langa, C. and Bernabéu, C. (1994). Phosphorylation of the human-transforming-growth-factor-beta-binding protein endoglin. *Biochem. J.* **301**, 765-768.
Lastres, P., Letamendía, A., Zhang, H., Rius, C., Almendro, N., Raab, U., López, L. A., Langa, C., Fabra, A., Letarte, M. et al. (1996). Endoglin modulates cellular responses to TGF-beta 1. *J. Cell Biol.* **133**, 1109-1121.
Li, W. (2013). Phagocyte dysfunction, tissue aging and degeneration. *Ageing Res. Rev.* **12**, 1005-1012.
Liu, Y., Jovanovic, B., Pins, M., Lee, C. and Bergan, R. C. (2002). Over expression of endoglin in human prostate cancer suppresses cell detachment, migration and invasion. *Oncogene* **21**, 8272-8281.
Lloberas, J. and Celada, A. (2002). Effect of aging on macrophage function. *Exp. Gerontol.* **37**, 1325-1331.
Llorca, O., Trujillo, A., Blanco, F. J. and Bernabeu, C. (2007). Structural model of human endoglin, a transmembrane receptor responsible for hereditary hemorrhagic telangiectasia. *J. Mol. Biol.* **365**, 694-705.
López-Novoa, J. M. and Bernabeu, C. (2010). The physiological role of endoglin in the cardiovascular system. *Am. J. Physiol.* **299**, H959-H974.
Mahbub, S., Deburghgraeve, C. R. and Kovacs, E. J. (2012). Advanced age impairs macrophage polarization. *J. Interferon Cytokine Res.* **32**, 18-26.
Mantovani, A., Sica, A., Sozzani, S., Allavena, P., Vecchi, A. and Locati, M. (2004). The chemokine system in diverse forms of macrophage activation and polarization. *Trends Immunol.* **25**, 677-686.
O'Connell, P. J., McKenzie, A., Fisicaro, N., Rockman, S. P., Pearse, M. J. and d'Apice, A. J. (1992). Endoglin: a 180-kD endothelial cell and macrophage restricted differentiation molecule. *Clin. Exp. Immunol.* **90**, 154-159.
Okuma, E., Saeki, K., Shimura, M., Ishizaka, Y., Yasugi, E. and Yuo, A. (2000). Induction of apoptosis in human hematopoietic U937 cells by granulocyte-macrophage colony-stimulating factor: possible existence of caspase 3-like pathway. *Leukemia* **14**, 612-619.
Oliveros, J. C., Blaschke, C., Herrero, J., Dopazo, J. and Valencia, A. (2000). Expression profiles and biological function. *Genome Inform. Ser. Workshop* **11**, 106-117.
Pello, O. M., Silvestre, C., De Pizzol, M. and Andrés, V. (2011). A glimpse on the phenomenon of macrophage polarization during atherosclerosis. *Immunobiology* **216**, 1172-1176.
Pérez-Gómez, E., Eleno, N., López-Novoa, J. M., Ramirez, J. R., Velasco, B., Letarte, M., Bernabéu, C. and Quintanilla, M. (2005). Characterization of murine S-endoglin isoform and its effects on tumor development. *Oncogene* **24**, 4450-4461.
Phillips, D. J., de Kretser, D. M. and Hedger, M. P. (2009). Activin and related proteins in inflammation: not just interested bystanders. *Cytokine Growth Factor Rev.* **20**, 153-164.
Plowden, J., Renshaw-Hoelscher, M., Engleman, C., Katz, J. and Sambhara, S. (2004). Innate immunity in aging: impact on macrophage function. *Aging Cell* **3**, 161-167.
Racioppi, L. and Means, A. R. (2012). Calcium/calmodulin-dependent protein kinase kinase 2: roles in signaling and pathophysiology. *J. Biol. Chem.* **287**, 31658-31665.
Rana, S., Cerdeira, A. S., Wenger, J., Salahuddin, S., Lim, K. H., Ralston, S. J., Thadhani, R. I. and Karumanchi, S. A. (2012). Plasma concentrations of soluble endoglin versus standard evaluation in patients with suspected preeclampsia. *PLoS ONE* **7**, e48259.
Robson, N. C., Phillips, D. J., McAlpine, T., Shin, A., Svobodova, S., Toy, T., Pillay, V., Kirkpatrick, N., Zanker, D., Wilson, K. et al. (2008). Activin-A: a novel dendritic cell-derived cytokine that potently attenuates CD40 ligand-specific cytokine and chemokine production. *Blood* **111**, 2733-2743.
Rulo, H. F., Westphal, J. R., van de Kerkhof, P. C., de Waal, R. M., van Vlijmen, I. M. and Ruiter, D. J. (1995). Expression of endoglin in psoriatic involved and uninvolved skin. *J. Dermatol. Sci.* **10**, 103-109.
Scutera, S., Riboldi, E., Daniele, R., Elia, A. R., Fraone, T., Castagnoli, C., Giovarelli, M., Musso, T. and Sozzani, S. (2008). Production and function of activin A in human dendritic cells. *Eur. Cytokine Netw.* **19**, 60-68.
Shaw, A. C., Joshi, S., Greenwood, H., Panda, A. and Lord, J. M. (2010). Aging of the innate immune system. *Curr. Opin. Immunol.* **22**, 507-513.
Shovlin, C. L. (2010). Hereditary haemorrhagic telangiectasia: pathophysiology, diagnosis and treatment. *Blood Rev.* **24**, 203-219.
Sierra-Filardi, E., Puig-Kröger, A., Blanco, F. J., Nieto, C., Bragado, R., Palomero, M. I., Bernabéu, C., Vega, M. A. and Corbí, A. L. (2011). Activin A skews macrophage polarization by promoting a proinflammatory phenotype and inhibiting the acquisition of anti-inflammatory macrophage markers. *Blood* **117**, 5092-5101.
Sozzani, S. and Musso, T. (2011). The yin and yang of Activin A. *Blood* **117**, 5013-5015.
Sunderkötter, C., Steinbrink, K., Goebeler, M., Bhardwaj, R. and Sorg, C. (1994). Macrophages and angiogenesis. *J. Leukoc. Biol.* **55**, 410-422.
Torsney, E., Charlton, R., Parums, D., Collis, M. and Arthur, H. M. (2002). Inducible expression of human endoglin during inflammation and wound healing in vivo. *Inflamm. Res.* **51**, 464-470.

Journal of Cell Science

Valbuena-Diez, A. C., Blanco, F. J., Oujo, B., Langa, C., Gonzalez-Nuñez, M., Llano, E., Pendas, A. M., Díaz, M., Castrillo, A., Lopez-Novoa, J. M. et al. (2012). Oxysterol-induced soluble endoglin release and its involvement in hypertension. *Circulation* **126**, 2612-2624.

Velasco, S., Alvarez-Muñoz, P., Pericacho, M., Dijke, P. T., Bernabéu, C., López-Novoa, J. M. and Rodríguez-Barbero, A. (2008). L- and S-endoglin differentially modulate TGFbeta1 signaling mediated by ALK1 and ALK5 in L6E9 myoblasts. *J. Cell Sci.* **121**, 913-919.

Werner, S. and Alzheimer, C. (2006). Roles of activin in tissue repair, fibrosis, and inflammatory disease. *Cytokine Growth Factor Rev.* **17**, 157-171.

Wilm, M., Shevchenko, A., Houthaeve, T., Breit, S., Schweigerer, L., Fotsis, T. and Mann, M. (1996). Femtomole sequencing of proteins from polyacrylamide gels by nano-electrospray mass spectrometry. *Nature* **379**, 466-469.

Yu, J., Shao, L. E., Frigon, N. L., Jr, Lofgren, J. and Schwall, R. (1996). Induced expression of the new cytokine, activin A, in human monocytes: inhibition by glucocorticoids and retinoic acid. *Immunology* **88**, 368-374.

SUPPLEMENTARY MATERIAL

EXPRESSION OF ENDOGLIN ISOFORMS IN THE MYELOID LINEAGE AND THEIR ROLE DURING AGING AND MACROPHAGE POLARIZATION

Mikel Aristorena[1,2], Francisco J. Blanco[1,2], Mateo de Las Casas-Engel[1], Luisa Ojeda-Fernandez[1,2], Eunate Gallardo-Vara[1,2], Angel Corbi[1], Luisa M. Botella[1,2], Carmelo Bernabeu[1,2]

[1]Centro de Investigaciones Biológicas, Consejo Superior de Investigaciones Científicas (CSIC), and [2]Centro de Investigación Biomédica en Red de Enfermedades Raras (CIBERER), 28040 Madrid, Spain

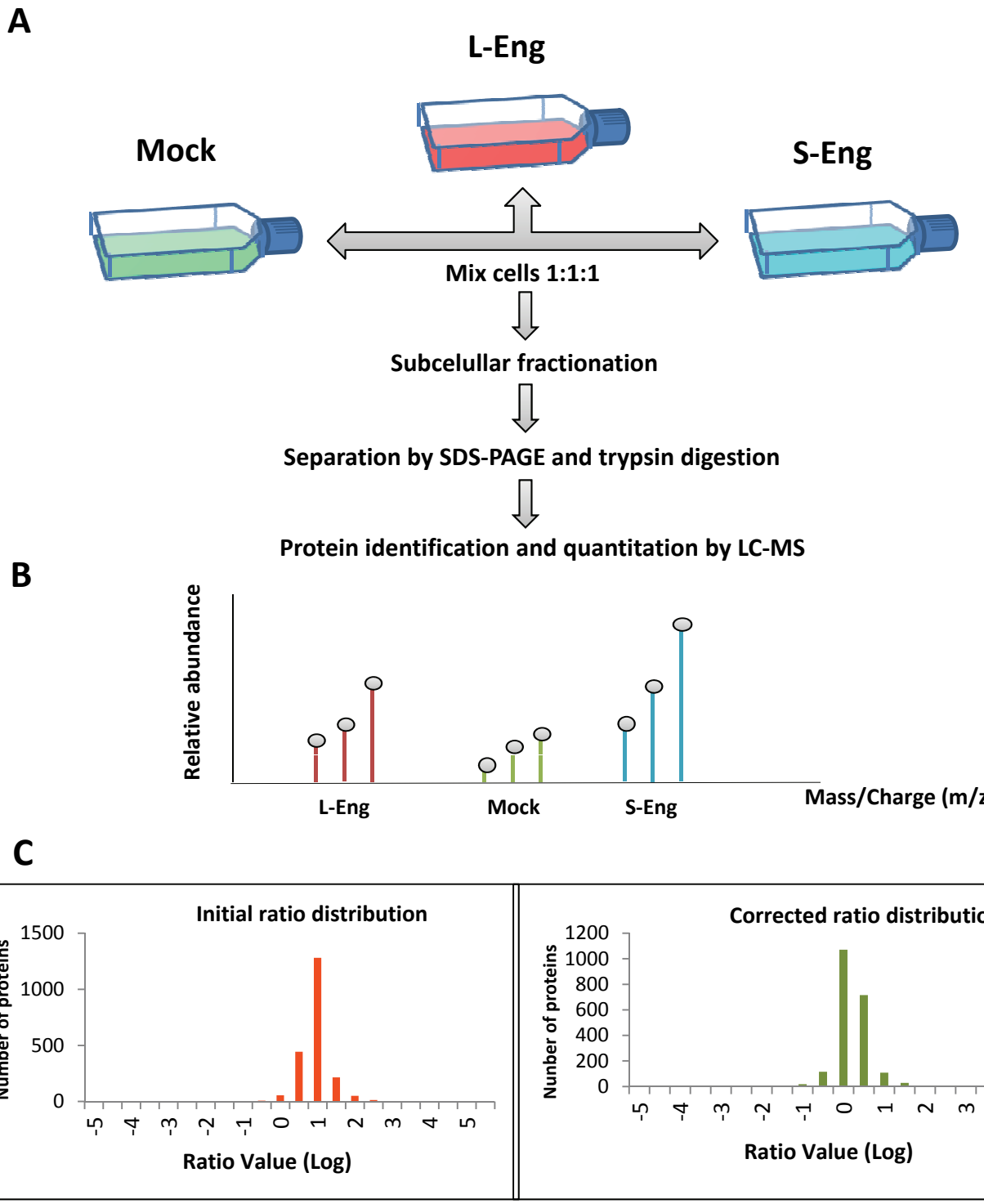

Suplementary Figure 1

L-Endoglin

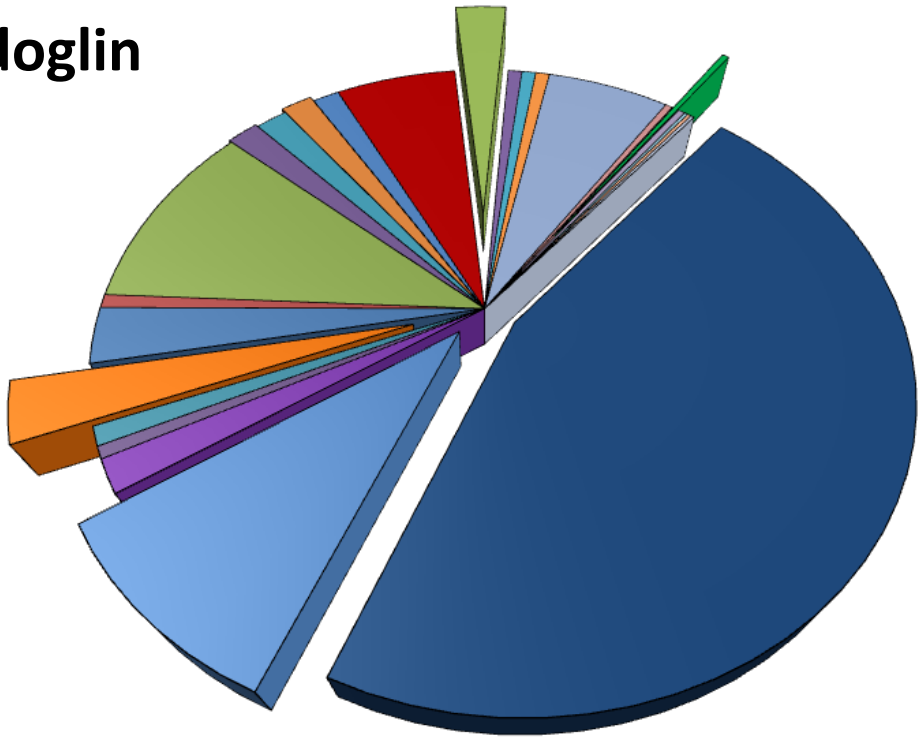

- Cell Death and Survival *
- Cellular Growth and Proliferation *
- Cellular Assembly and Organization
- Cellular Function and Maintenance
- Cellular Compromise
- Free Radical Scavenging #
- DNA Replication, Recombination, and Repair
- Amino Acid Metabolism
- Infectious Disease
- Developmental Disorder
- Hereditary disorder
- Respiratory Disease
- Immunological Disease
- Cancer
- Cell Cycle *
- Gastrointestinal Disease
- Molecular Transport
- Small Molecule Biochemistry
- Hematological Disease
- Cell-To-Cell Signaling and Interaction
- Immune Cell Trafficking *
- RNA Post-Transcriptional Modification
- Carbohydrate Metabolism
- Connective Tissue Development and Function
- Skeletal and Muscular System Development

S-Endoglin

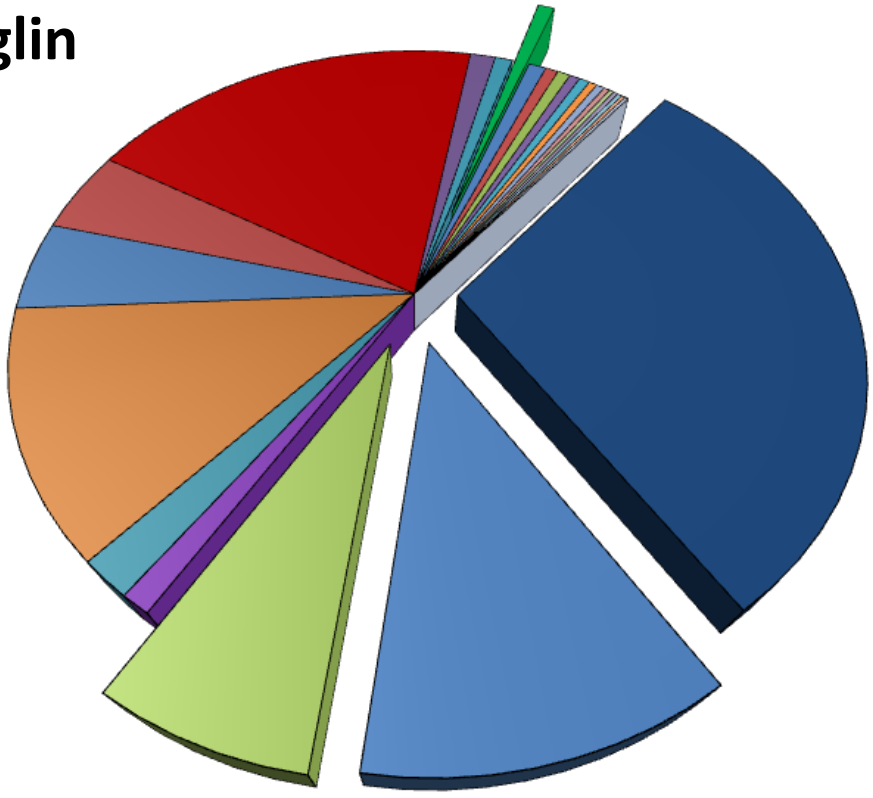

- Cell death and Survival *
- Cellular Growth and Proliferation *
- Cell Cycle*
- Cellular Assembly and Organization
- DNA Replication, Recombination, and Repair
- Hematological Disease
- Infectious Disease
- Cellular Development
- Cancer
- Cellular Movement
- Cell-To-Cell Signaling and Interaction
- Immune Cell Trafficking *
- Tissue Development
- Connective Tissue Disorders
- Skeletal and Muscular Disorders
- Dental Disease
- Gastrointestinal Disease
- Post-Translational Modification
- Protein Folding
- Hypersensitivity Response
- Dermatological Diseases and Conditions
- Developmental Disorder
- Hereditary Disorder
- Cell Morphology
- Gene Expresion

Supplementary Figure 2B

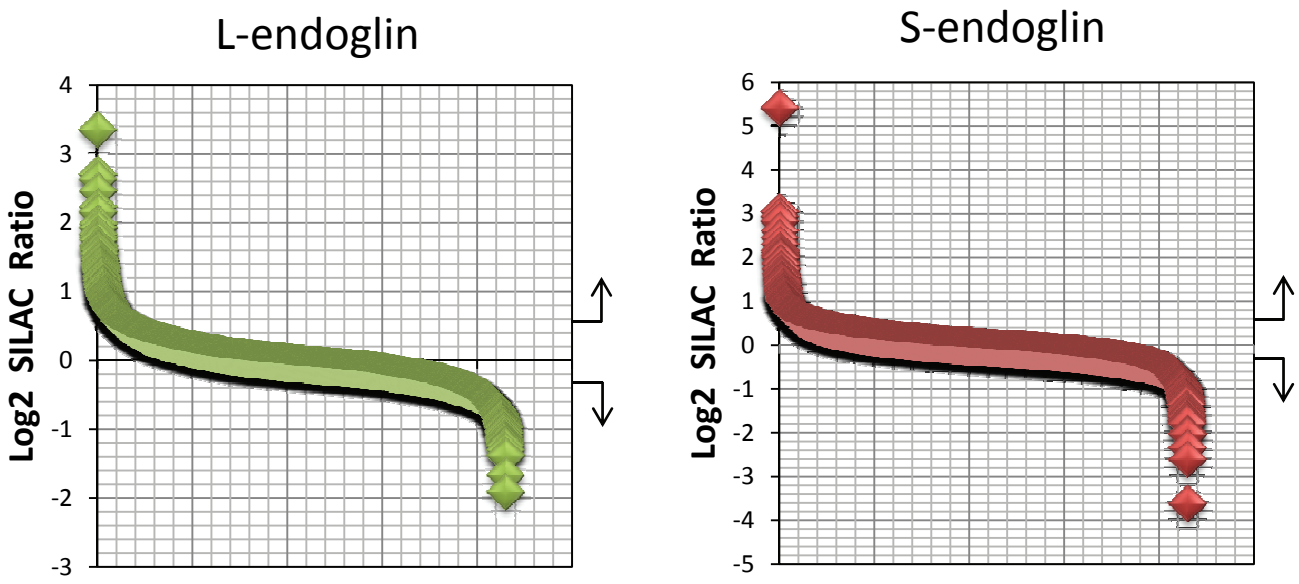

Supplementary Figure 3

SUPPLEMENTARY FIGURE LEGENDS

Supplementary Figure 1. SILAC labelling and analysis strategy in endoglin monocytic transfectants. U937 transfectants were harvested and labelled with light (Lys, Arg; C12), medium (Lys, Arg; C13) and heavy (Lys, Arg; C13-N15) amino acids by culturing in SILAC media. Equal number of cells, in different combinations, were mixed, lysed and fractionated for individual membrane, cytoplasm and nuclear analysis using SDS-PAGE followed by trypsin digestion. Then, protein identification and quantitation was carried out by liquid chromatography and mass spectroscopy (LC-MS) (**A**). Light, medium and heavy spectra of the peptides was obtained in an LTQ Orbitrap equipment and analysed to get the protein level ratios based on the detected relative abundance (**B**). Labelling efficiency was checked and ratios where manually normalized in all subcellular fractions to correct the mixing-labelling variability (**C**).

Supplementary Figure 2. Ingenuity pathway analysis of SILAC proteome list. The bio-informatic Ingenuity Pathways Analysis (IPA) of the final protein list obtained after SILAC analysis is shown. The Ingenuity Knowledge Base (Genes Only) was used as a reference set. Direct and indirect relationships for human genes with high confidence in experimentally observed interactions were analyzed. Predicted networks (with high confidence) were also checked. Top 25 significantly altered biofunctions are shown for L-endoglin (**A**) and S-endoglin (**B**) U937 transfectants respect to mock controls. *Illustrative common biofunctions affected in both transfectants; #Example of specific biofunction affected in L-endoglin transfectants. The list of biofunctions is ordered from top to bottom according to their statistical significance (between $p<1.19x10^{-9}$ and $p<2.98x10^{-2}$). The area in the pie diagram relates to the number of altered proteins in each biofunction.

Supplementary Figure 3. **Quantitative analysis of protein expression in endoglin U937 transfectants.** Logarithmic ratio distribution of the SILAC raw data after normalization respect to mock transfectants. Most of the identified proteins for both transfectants (>4,000) have a value close to zero. Broken arrows indicate the approximate cut-off values (0.585 and -0.322).

Supplementary Table 1. List of differentially expressed proteins obtained from SILAC analysis.

Download Table S1

Supplementary Table 2. SILAC ratios of the top ten most deregulated proteins in L-endoglin and S-endoglin transfectants.

L-Endoglin

UP

Proteins	Ratio
MARS2	2.875
ARRB1	2.853
CTSG*	2.808
PSTPIP2*	2.133
DAK	1.974
IL4I1	1.887
SRP54	1.827
NR2F2	1.762
CST7*	1.711
PSTPIP1	1.680

DOWN

Proteins	Ratio
LRPAP1*	-1.260
TES	-1.248
UBASH3B	-1.239
APPL1	-1.229
VIM*	-1.220
LIG1*	-1.220
DHPS	-1.209
FBXO4	-1.208
RPL15	-1.202
DCTPP1*	-1.143

S-Endoglin

UP

Proteins	Ratio
CTSG*	2.817
PRTN3*	2.687
PSTPIP2*	2.435
SRP19	2.293
TRIM27	2.026
CDA	1.980
NR2F2	1.633
COPS5	1.419
C11orf31	1.410
CST7*	1.381

DOWN

Proteins	Ratio
ANXA2*	-1.810
UBASH3B	-1.678
GGCT	-1.556
RAB27B	-1.393
CC2D1A	-1.335
CTR9	-1.292
S100A11	-1.266
IQGAP3	-1.262
LIG1*	-1.239
BRD3	-1.218

Logarithmic SILAC ratios are shown. Asterisks indicate proteins down- or up-regulated in both endoglin transfectants. Please note that not all the marked proteins of a given transfectant are shared in the top ten list of the other one (See Supplementary Figure 1). **ANXA2**, Annexin A2; **APPL1**, DCC-interacting protein 13-alpha; **ARRB1**, Beta-arrestin-1; **BRD3**, Bromodomain-containing protein 3; **C11orf31**, Uncharacterized protein C11orf73; **CC2D1A**, Coiled-coil and C2 domain-containing protein 1A; **CDA**, Cytidine deaminase; **COPS5**, COP9 signalosome complex subunit 5; **CST7**, Cystatin-F; **CSTG**, Cathepsin G; **CTR9**, RNA polymerase-associated protein CTR9 homolog; **DAK**, Bifunctional ATP-dependent dihydroxyacetone kinase/FAD-AMP lyase (cyclizing); **DCTPP1**, dCTP pyrophosphatase 1; **DHPS**, Deoxyhypusine synthase; **FBXO4**, F-box only protein 4; **GGCT**, Gamma-glutamylcyclotransferase; **IL4I1**, L-amino-acid oxidase; **IQGAP3**, Ras GTPase-activating-like protein IQGAP3; **LIG1**, DNA ligase 1; **LRPAP**, Alpha-2-macroglobulin receptor-associated protein; **MARS2**, Methionyl-tRNA synthetase mitochondrial; **NR2F**, COUP transcription factor 2; **NR2F2**, COUP transcription factor 2; **PRTN3**, Myeloblastin; **PSTPIP1**, Proline-serine-threonine phosphatase-interacting protein 1; **PSTPIP2**, Proline-serine-threonine phosphatase-interacting protein 2; **RAB27B**, Ras-related protein Rab-27B; **RPL15**, 60S ribosomal protein L15; **S100A11**, Protein S100-A11; **SRP19**, Signal recognition particle 19; **SRP54**, Signal recognition particle 54 kDa protein; **TES**, Testin; **TRIM27**, Zinc finger protein RFP; **UBASH**, Ubiquitin-associated and SH3 domain-containing protein B; **UBASH3B**, Ubiquitin-associated and SH3 domain-containing protein B; **VIM**, Vimentin.